Pyrolysis technology for *Cortaderia selloana* invasive species. Prospects in the biomass energy sector.

Alejandro Pérez[1], Begoña Ruiz[1], Enrique Fuente[1], Luis Fernando Calvo[2*], Sergio Paniagua[2].

[1]Biocarbon and Sustainability Group (B&S), Instituto de Ciencia y Tecnología del Carbono, INCAR-CSIC. Francisco Pintado Fe, 26. 33011 Oviedo, Spain.

[2] University of León, Department of Chemistry and Applied Physics, Chemical Engineering Area, IMARENABIO, Avda. Portugal 41 (24071), León, Spain.

* Corresponding author email: lfcalp@unileon.es. Telephone: +34 987291843

ABSTRACT

Cortaderia selloana (CS), is an invasive and exotic species that is generating significant invasive problems in the Iberian Peninsula ecosystems. The objective of this research was to study this plant potential thorough a pyrolytic process helping to reduce its expansion. Stems and leaves were subjected to conventional and flash pyrolysis. These processes were carried out in an original design oven using a 25°C/min heating ramp at a 750°C temperature and during 60 min at the pyrolysis temperature for conventional pyrolysis and with 750°C and 850°C pyrolysis temperatures for flash. Gas-fraction obtained by flash pyrolysis had higher HHV data when compared with conventional ones (~17 MJ/kg *vs* ~ 5 MJ/kg) due to their less CO_2 and higher CO, CH_4 and H_2. The greater bio-oil yield was obtained for CSS-P (33.58%). The composition of conventional pyrolysis bio-oils had an overbearing of nonaromatic and monoaromatic hydrocarbons nature whereas bio-oils from flash pyrolysis were composed mainly of polycyclic aromatic hydrocarbons. Bio-char fraction was higher in CSL than CSS with HHV similar to lignite and bituminous coals (22.74 to 29.12 MJ/kg). After done the quantification and characterization of the fractions, it was concluded that a possible energetic valorization of *Cortaderia selloana* biomass was possible.

KEYWORDS

Bio-char; bio-fuel; *Cortaderia selloana* biomass; flash pyrolysis; pampa grass invasive species; pyrolysis technology.

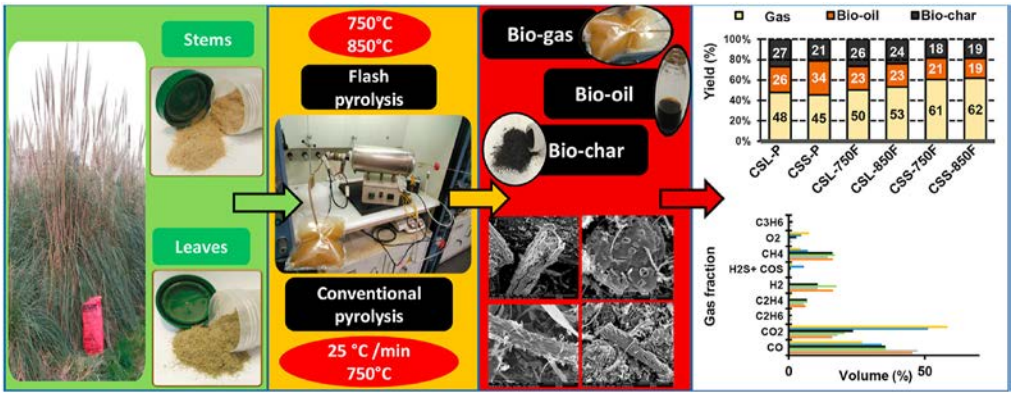

Highlights:

- Valorization of invasive pampa grass (Cortaderia selloana) by pyrolysis technology.
- Different HHV for flash and conventional pyrolysis bio-oils (~33 MJ/kg vs ~23 MJ/kg).
- Gas is the main fraction of the flash and conventional pyrolysis (up to 62%).
- Flash pyrolysis promotes a biogas with more CH_4, H_2, CO and synthesis gas content.
- Bio-chars from stems present a HHV (up to 29 MJ/kg) in the order of bituminous coals.

1. INTRODUCTION.

The faster population growth as well as the development of the world economy are causing energy demand to grow at an exponential rate. In this scenario, fossil fuels are, at present, the main energy source [1]. The widespread use of petroleum products has been dramatically increasing in recent years [2]. All fossil and mineral fuels are finite and non-renewable, so different research on renewable energy is being developed.

Currently, the circular economy plays an increasingly important role in scientific investigations with aim is the energy obtention [3], and therefore, renewable energies are one of the most viable alternatives that allow a more economical, clean and sustainable energy. Biomass is a potential CO_2-neutral, clean and sustainable energy resource [4]. It is known that biomass energy reduces greenhouse gas emissions [2] in the same way that raw biomass co-firing with coal causes lower emissions of CO_2, SO_2 and nitrogen oxides (NO_x) when compared with coal-torrefied biomass blends [5]. This study focused on the use of biomass for energy production, specifically, the species *Cortaderia selloana* (Schult. & Schult. f.) Asch. & Graebn., commonly known as pampa grass, was used as renewable energy source. This plant, originally from Latin America (Argentina, Chile, Brazil and Uruguay) [6,7] is currently one of the main invasive species in southern Europe [8] colonizing disturbing places in a short time [9] and generating large vegetative tussocks and tall, persisting flowering heads [10]. This way, the use of this species aerial parts for energy purposes could be an attractive option. It is also known that it can biomineralise abundant quantities of silica in its tissues in the form of silicophytoliths [11]. At present, the pampa grass is considered “invasive species” with strong dominance that can become invasive on important native ecosystems [7]. This situation causes a problem which is especially critical in the southern of Europe and, particularly, in the North West of Spain [10]. It drastically negative influents both the species richness, community evenness and richness [12]. The most effective method for controlling this problem is to cut or prune the invasive plan, something that generates large amounts of waste with no use or value [13]. Hence, *Cortaderia selloana (CS),* could be a biomass source for energy purposes and it could also be a temporary alternative of energy crops such as plant of the genus *Miscanthus* [14] or the canola (*Brassica napus)* [15,16]. Until now, it has been little studied in the field of waste valorization and there are only a few research related to this

biomass as adsorbent material [6,17–19]. This study constitutes a first approach to the possible energy use of biomass from this invasive plant, pampa grass.

The different ways to transform biomass using thermochemical conversion are: combustion, gasification and pyrolysis [4,20]. In pyrolysis process the raw material is subjected to high temperature in oxygen-limited environment. The main goal of the pyrolysis process is the conversion of the largest possible part of the input material to obtain solid or carbonised products, liquid products (bio-oils, tars, and water) and a gas mixture composed mainly of CO_2, CO, H_2, and CH_4 [21–23]. Often, the process is also pursued to get the highest possible yield of a selected fraction [24]. The proportions and composition of the pyrolysis products before mentioned rely on the conditions used [1]. The experimental pyrolysis variables are (among others): heating rate, temperature, residence time, gas flow and material granulometry. Depending on the heating rate, pyrolysis can be classified into three different types: slow, rapid and flash pyrolysis. Regarding the type of pyrolysis used and the structure and chemical composition of the biomass, the production of bio-char, bio-oil or gas can be maximized. From the optimization process, developing models for simulating biomass pyrolysis becomes increasingly important [25]. Slow or conventional pyrolysis are characterized by very slow heating rates resulting a higher amount of pyrolyzed solids or bio-chares. Concerning fast and flash pyrolysis, recent literatures have shown higher yields of primary, non-equilibrium liquids, and gases, including valuable chemicals, petrochemicals, chemical intermediates, and fuels obtained from the biomass feedstocks [26].

After a detailed study of the state of the art, and after the previous research carried out by the work team related to the pyrolytic conversion of agricultural biomass [2], the potential of the pampa grass to obtain good yields in its energy conversion was established as working hypothesis. This way, apart from the energy aspects, a solution was offered for the use of the residues of this invasive species.

Hence, in this research, authors studied the pyrolytic process of the stems and leaves derived from *Cortaderia selloana* invasive plant. Both conventional and flash pyrolysis were carried out analysing the different solid (SEM-EDX) and liquid-gas (chromatographic analysis) fractions. In the same sense, and apart from the yields identification for the different fractions, a

thermogravimetry study of raw biomass (TGA) together with the determination of the inorganic composition of the biomass (ICP-MS) was also done for the ashes.

Therefore, a double objective was proposed to be achieved in this research. On the one hand, to study the behaviour of the biomass considered when it was subjected to pyrolysis processes, studying the kinetics of the heating process under an inert atmosphere and, on the other hand, to study the proportion and composition of the different fractions (biochar, biogas and biooils) obtained in the process.

2. MATERIAL AND METHODS.

2.1. Raw material sampling, pretreatment and size reduction.

The biomass collection, stems and leaves of Pampa grass CS, was carried out in an urban area of the Council of Avilés, Asturias, Spain.

The biomass was cut to reduce its size (up to 1-2 cm). Subsequently, the samples were dried in a drying room for 4 days at 40°C until constant weight. Later, a second reduction in size to 0.5 mm was done to obtain a homogeneous material with an optimum particle size for subsequent analyzes and processes. The total sample was divided by quartering method and with a divisor of parallel and equidistant partitions walls to obtain sub-samples which quantities are able to manage under laboratory conditions.

A scheme of the sample preparation is shown on **Appendix A-Supplementary Data.**

2.2. Characterization of the samples.

2.2.1. Chemical characterization.

The carbon (C), hydrogen (H) and nitrogen (N) contents were determined using a LECO CHN-2000 equipment according to ASTM D 5373. Determination of the Sulphur (S) content was carried out on a LECO S-144-DR instrument (LECO Corporation, Groveport, Ohio, United States), in accord with ASTM D 4239. The oxygen (O) content was calculated by difference. Related to proximate analysis, moisture and ash content were determined on a TGA 701 Leco in accordance with ASTM D 7582. Volatile matter was achieved according UNE 32019 norm. The high heating values (HHV) for both stems and leaves were done on a LECO AC-300. Using the data associated

with the elemental analysis, the calorific value (HHV) of the different fractions (bio-char, bio-oil and gas) was calculated. This way, Doulong-Petit [27], Eq. (1), and Beckman [28], Eq. (2), expressions were employed to estimate the HHV for bio-chars and bio-oils, respectively. Similarly, a series of material and energy balances have been needed to estimate the HHV of the gases.

$$HHV\ (kcal/kg) = 8140\ C + 34400\ (H-O/8) + 2220\ S \quad \text{Eq. (1)}$$

$$HHV\ (MJ/kg) = 0.352\ C + 0.994\ H + 0.105\ (S - O) \quad \text{Eq. (2)}$$

2.2.2. Inorganic composition of biomass by ICP-MS and XRF.

The inorganic composition of the biomass was determined in the ashes of the leaves and stems of CS by means of ICP–MS and XRF.

For ICP-MS analysis, ashes were digested in a microwave oven with a mixture of nitric and hydrochloric acids. The elemental analysis was carried out on an Agilent 7700x equipment.

For certain elements that could not be quantified with the ICP-MS, like silicon, X-ray Fluorescence (XRF) was used. The inorganic samples (0.50 g) were melted with 8.00 g of lithium tetraborate / lithium metaborate 66.00 % / 34.00 % (Equilab EQF-TML 66 / 34) at 1200°C for 12 minutes in a fusion machine (PERLX´3 - Philips). The resulting melt was transformed into a glass bead that was analyzed with a XRF spectrometer (SRS 3000 Bruker). The fluorescence intensities of the X-rays of the detected elements were measured in the bead.

2.2.3. Thermogravimetric analysis and kinetics.

Thermogravimetric analysis was carried employing a TGA instrument Q 5000IR. This instrument supplies a continuous measurement of sample weight as a function of time or temperature. Milled leaves and stems samples weighing around 14 – 25 mg were placed in a titanium crucible and heated under nitrogen atmosphere. Heating was carried out under a flow of 20 mL/min of N_2 under three different heating rates (5, 25 and 50°C/min) until reaching a temperature of 900°C (temperature at which they remained 15 minutes). This way, thermogravimetric profiles of the samples (TG) were obtained. To identify the different stages, it is advisable to derive these TG profiles (DTG profiles). With them, important parameters, as the temperature at which occur each stage as well as the mass loss, could be identified. Kinetic parameters (activation energy, E_a, and frequency factor, k_0) are very useful as a complement to the biomass samples analysis [29].

Activation energy (E_a) and frequency factor (k_0) values were estimated by approximate integral method, AIM, [30]. While E_a is associated with the energy required to start a chemical reaction, k_0 is the number of collisions between molecules involved in a reaction. The larger number of collisions, the higher the reaction rate. Because of that, k_0 is an essential parameter in interpreting temporary differences within DTG profiles. The kinetic parameters obtained for this study are those associated with the most representative peak of the active pyrolysis of each thermogravimetric profile.

2.3. Pyrolysis process

The methodology is based on previous experience of our research group with biomass pyrolysis processes as reported in the following published works [2,31], adapting it to an oven of original design. The original design experimental set-up (**Fig.1**) consisted of a horizontal tubular connected to a N_2 mass flow controller, a series of cooling condensers for capturing the bio-oils phase and Tedlar® sample bags (Supelco Analytical, USA) for retaining the gaseous phase. The furnace boundaries were isolated with ceramic refractory fibres to reduce heat losses. In addition, the part of the reactor outside the oven was coated with heating tapes. In this way, it was ensured that all bio-oils condensed in the heat exchanger and there were no remains at the end of the reactor or in the tubes connected to the condenser. The amount of sample used in each pyrolysis experiment was about 3 - 6 g for both stems and leaves. During the flash and the conventional pyrolysis, samples to be analysed were placed in an alumina crucible (Sigma-Aldrich, USA). The conventional pyrolysis experiment was done employing a flow of N_2 of 100 mL/min, a heating rate of 25°C/min rate, a pyrolysis temperature of 750°C and a final temperature time of 1 h. The gas and bio-oil fraction were collected in the temperature range between 200ºC and 550ºC (according to the temperature range in which biomass is devolatilized showed by thermogravimetric analysis), using an N_2 flow of 100 mL/min for 14 minutes. For its part, samples were introduced instantaneously into the furnace during the flash pyrolysis with a mechanical device when it reached the desired temperature (750 and 850°C). At that moment, the same N_2 flow was applied for 10 minutes. Dichloromethane (CH_2Cl_2) was used to extract the bio-oils from the condenser. The solution of CH_2Cl_2 and the bio-oils fraction was passed through a column filled with sodium sulphate anhydrous (Na_2SO_4). Then, the CH_2Cl_2 solutions and bio-oils were stored in glass

containers, sealed and refrigerated at a temperature of -3°C (optimal conditions to do the subsequent chromatographic analysis).

2.4. SEM-EDX.

The biomass and the bio-char obtained from the conventional and flash pyrolysis were examined using a scanning electron microscope, ZEISS Model DMS-942 (ZEISS, United States), equipped with an energy-dispersive X-ray analysis system (Link-Isis II). Prior to examination, samples were covered with iridium to decrease their charge and to improve the SEM pictures. An Emitech K575X instrument was employed for this purpose.

2.5. Chromatographic analysis.

The chromatographic analysis of gases fraction was performed on a GC System 7890A chromatograph (Agilent Technologies, Wilmington, DE, USA). The system has five valves and three detectors. The flame ionization detector (FID) was configured to analyse hydrocarbons since one to five carbons, while six and more carbons components were grouped and measured in a single peak at the beginning of the analysis. A thermal conductivity detector (TCD) with helium as reference gas or mobile phase was configured to analyse fixed gases (which may include CO_2, CO, O_2, N_2 or H_2S among others). Finally, the second TCD, with a reference N_2 gas, was used in the hydrogen analysis.

An Agilent 7890A chromatograph combined with a 5975C mass spectrometer (Agilent Technologies, Wilmington, DE, USA) was used for the bio-oil chromatographic analysis. An HP-5MS capillary column (Agilent Technologies, Wilmington, DE, USA) (5% phenyl-methylpolysiloxane) with dimensions of 30m x 0.25mm ID x 0.25µm, was employed to separate the compounds. The column was subjected to the following heating program: an initial temperature of 50°C, no dwell time, and a heating rate of 4 °C/min up to 300 °C. 1µl (split less) of the sample was injected into the equipment. The mass spectral libraries used for identifying the compounds included NIST08, Wiley7n and Wiley 275. The mass spectrometer was operated in full scan mode (50–550 uma, 3.21 scans/s, 70 eV ionization voltage). Before doing the analysis, the water presented in the bio-oils fraction was separated from the organic fraction.

3. RESULTS AND DISCUSSION.

3.1. Biomass chemical characterization.

Pampa grass leaves (CSL) and stems (CSS) characterization results appear in **Table 1**. The chemical analysis of both parts was so similar to other lignocellulosic biomass considered in different works [2,32]. Similarly, the C content of both parts (~47%) was higher than other biomass sources [33], what advances a good potentiality in its energy conversion, but far away for carbon content in coals [34]; being a common characteristic in the use of biomass as energy sources. The difference found considering the nitrogen (N) content between stems and leaves was due to a competitive CS strategy. The plants of this species accumulate this element in their leaves from their dead leaves [9]. There is also a clear difference in CSL (7.5%) and CSS (2.5%) ash content due mainly to the higher silica content in this biomass (4.40% *vs* 1.40%), which presence increases the ash fraction in biomass samples. This fact could cause by the high foliar content of silicophytoliths [35]. Silicophytoliths have been widely studied and it has been proven that, thanks to them, different plants can bioaccumulate large quantities of a higher number of elements, including Sulphur [11]. The CSL ash percentage was higher than this same biomass source derived from the work of Lanning and Eleuterius [36]. This is so because in the aforementioned study, CS plants were in a natural area and with a wide availability of resources. Under these conditions, pampa grass does not produce as much silicophytoliths, opting to generate lignin [37]. CCS ashes values were in line with cereals straw [38]. On the other hand, the CSS ash content (2.5%) was similar to that obtained for this same invasive species in natural environment [36]. Regarding volatile matter, stems showed higher values than leaves (81.9% *vs* 74.8%); these values were so similar to the obtained ones for other similar biomass [39,40]. Finally, and related to HHV, both stems and leaves had similar HHV results (~ 19 MJ/kg). They were similar to woody biomass [4] and lower than fossil fuels [41].

3.2. ICP-MS and X-ray fluorescence.

The chemical elements viability in a soil is high and plants tend to accumulate them in different tissues [42]. Ashes ICP-MS analysis of CSS and CSL is shown in **Fig. 2**. CSS (**Fig. 2.a**) and CSL (**Fig. 2.b**). Both analyses showed potassium (K), calcium (Ca), sulphur (S), magnesium (Mg) and sodium (Na) as the major elements. Ash-related issues such as slagging, agglomeration and

corrosion are severe limitations in combustion [43,44]. K, Na, Ca and Mg bear the primary responsibility for the above issues [45]. K and Ca were the elements with higher concentrations for the analysed *C. selloana* ashes biomass samples. The high content of them is unfavorable, since they can easily react with other elements (e.g., Si) to form alkali with very low melting points (700 °C). Increased K content may increase the slag potential of deposits. Whereas ashes with less alkali and with higher Ca contents exhibit more manageable slagging, fouling, and corrosion problems [46]. For CSL and CSS the analysed elements ranked by decreasing content in the examined ashes were: Ca>K>S>Mg>Na. These composition was so similar to the obtained for forest residues [47] except for the Mg and Na elements.

This is a common trend, since plant biomass is mainly composed of alkaline and alkaline earth compounds [48]. Some metals were also detected in lower concentrations (CSS: 546 ppm Mn and 226 ppm Cu and CSL: 651 ppm Li and 320 ppm Mn). There was, therefore, a differentiation between the leaves and stems in terms of their chemical elements composition. CSL showed higher concentrations of P and Li. On the other hand, CSS had higher concentrations of S and Mg. The greater presence of P in CSH is a direct cause of the greater amount of silicon present in this biomass [49].

The X-ray fluorescence analysis determined a series of oxides present in the CSS and CSL biomass ashes. For all of them, only silicon oxides (SiO_2) were considered due to the other oxides may have volatilized in the pearl formation process, where the samples were subjected to a temperature of 1200 ºC [50]. Data obtained for SiO_2 in ashes were 56.5% and 59.5%, respectively (SiO_2 in CSS and CSL biomass were 1.4% and 4.4%, respectively). These results were higher when compared to the Lanning and Eleuterius [36] works. Furthermore, they were also higher than the obtained for the same species in the Honaine et al [11] and also superior than the achieved by Wang et al [51] for barley straw and husk.

3.3. Pampa grass TGA and kinetics.

The thermogravimetric profiles are shown in **Fig. 3.** In the same way, DTG characteristic parameters are shown in **Table 2**. Results obtained for stems and leaves biomass were in line with the typical profiles for biomass pyrolysis [52] and, specifically, with another woks that allude

to this grass [13]. The thermogravimetric curves of the CSS and CSL biomass decomposition are very similar as can be seen in **Fig. 3** and the percentage of final weight loss was independent of the heating rate. These profiles were related to the samples degradation of hemicellulose, cellulose and lignin. Although hemicellulose and cellulose have quite defined decomposition moments (between 150-350°C and 275-350ºC, respectively), the lignin, in contrast, has a very wide range of degradation (250-500ºC) which is completely overlapped with the previous components decomposition [52]. For all the heating rates (5, 25 and 50 ºC/min) maximum DTG values were higher for stems (characterized by a higher C content). As can be seen, the highest DTG_{max} values were reached at a heating rate of 5 °C / min, which were also obtained at the lower temperatures.

The kinetics results are shown in **Table 2**. CSL presented lower E_a values (154.83-168.17 kJ/mol) than CSS (222.85-292.84 kJ/mol), which means that the beginning of the biomass decomposition in the pyrolytic process requires less energy as a consequence of its lower lignin content. The decomposition of the pampa grass biomass associated with the lower E_a values also occurred at lower T_{DTGmax} range. This means a lower energy outlay for the lowest heating rate (5 ºC/min). The frequency factor parameter, k_0, is linked to the rate at which chemical reactions develop. The fastest matter release was obtained for CSS, especially with a heating rate of 25 and 50 °C/min. Regarding CSL, there was more homogeneity in the k_0 results. CSS showed similar E_a and k_0 values in relation to those presented for the woody biomass [53]. For its part, CSL values were so similar to the husk and rice straw [54].

3.4. Pyrolytic process.

3.4.1. Yield.

Results associated with yield values of the pyrolysis processes appear in **Fig. 4.** For flash pyrolysis, the gas fraction was predominant (up to 61.98%). The bio-oil fraction decreases slightly with the increase of the flash pyrolysis temperature and independently of the biomass type (CSL 23.36% *vs* 22.96% and CSS 21.33% *vs* 19.35% for 750 ºC and 850 ºC, respectively). CSL biomass produced a higher bio-char fraction (26.48% and 23.93%) than CSS biomass (~18.5%, with the only exception of CSS-P). In the study of Sun et al. [55] about flash pyrolysis at 700ºC and 800ºC, authors obtained values for gas, bio-oil and bio-char yields around 30-40% working

with rice husk. In this work the bio-oils yield was similar to the bio-oil yield of CSS-P. In contrast, in the study by Maliutina et al. [56]; they worked with the palm kernel shell flash pyrolysis, bio-oils were the main fraction (higher than 65 %) and bio-char and biogas fractions did not reach values greater than 20%.

Also, during conventional pyrolysis, the biogas fraction was highlighted as the majority fraction (47.75 % and 45.43 % for CSL-P and CSS-P, respectively) although these yields were slightly lower than those obtained for the flash pyrolysis. These results were over the typical values in a slow pyrolysis (~35%) [57]. Bio-oils fraction obtained for both biomass (25.51 % and 33.68 % for CSL-P and CSS-P respectively) were higher than those obtained working with flash pyrolysis. Like in the flash pyrolysis, CSL biomass produced a larger fraction of bio-char (26.74% and 20.99% for CSL-P and CSS-P respectively).

Compared to same experiment designed with pomegranate peel [2], it was noted several yield differences. In general, gas yields were smaller for pomegranate peel (~36 % for slow pyrolysis al 750 ºC; ~16 % and ~50 % for flash pyrolysis at 750 ºC and 850 ºC) whereas bio-oil yield was greater (~35 % for slow pyrolysis al 750 ºC; ~53 % and ~24 % for flash pyrolysis at 750 ºC and 850 ºC).

The obtained results validate the initial hypothesis raised, verifying the possibility of conversion of CS through flash pyrolysis processes, in different fuels (bio-char, gas, bio-oil).

3.4.2. Gas fraction.

After the gas chromatographic analysis (**Fig. 5**), differences in biogas composition with respect to flash and conventional pyrolysis were observed. Flash pyrolysis showed high amounts of CO (up to 47.19%), CH_4 (up to 16.97%) and H_2 (up to 17.5%) as well as moderate amounts of ethylene (C_2H_4) (up to 6.97%); CO_2 concentrations were much lower in flash pyrolysis (<25 %) than those present in conventional pyrolysis (up to 58 %). The use of a higher temperature in the flash pyrolysis process (850ºC *vs* 750ºC) involved a greater H_2 and CH_4 formation (syngas) in the same way that it maintained the CO content and decreased the CO_2 content in the biogas, regardless of the type of biomass studied (CSS and CSL). The gas of the CSS biomass flash pyrolysis contained higher amounts of CO (47% and 45% in CSS-750F and CSS-850F *vs* ~36% in CSL-750F and CSL-850F), which is consistent with the analytical results of this biomass sample,

characterized by a higher content of C, while, for their part, the H_2, CH_4 and C_2H_4 content were very similar. The flash pyrolysis for palm kernel shell [56] generated a great amount of CO (up to 60%) followed by H_2 (up to 22%) and low values for CO_2 (up to 10%). The flash pyrolysis of the pomegranate peel under the same conditions [2] produced a gas fraction with higher CO_2 content (~35 %) and lower CO (~33 %) and CH4 (up to ~12%). After comparing these data, it can be stated that the biomass nature influenced the gas composition.

Regarding to conventional pyrolysis, the CSS and CSL gas composition produced high CO_2 content (up to 58%), close to twice that obtained in flash pyrolysis, moderate CO (up to 34%) and CH_4 content (up to 7%) and a negligible amount of H_2. Pomegranate peel under the same conditions [2] produced a gas fraction with higher CO_2 content (~67 %) and lower CO content but a slightly amount of H_2 (~5%). CO_2 and CO were produced by hemicellulose and cellulose due to the thermal decomposition of their carbonyl and carboxyl groups. Lignin produced light hydrocarbons (such as CH_4) and H_2 because the thermal degradation of its methoxy / methylene groups and aromatic rings [4,57].

Table 3 shows the HHV for the gas samples obtained from CSS and CSL by the different pyrolysis technologies. For both, there was a relevant difference between the HHV values obtained for the gases by conventional pyrolysis (~5 MJ/kg) and flash pyrolysis (~17 MJ/kg). The HHV increased as the flash pyrolysis temperature did; this could be due to the increase in the H_2 volume. CSL-850F (flash pyrolysis at 850 ºC) was the gas fraction with higher HHV value (17.18 MJ/kg). The pomegranate peels gas fraction achieved by conventional and flash pyrolysis [2] showed lower HHV values (3.6 MJ/kg and 11.5 MJ/kg, respectively). This great yield reached during flash pyrolysis together with their high HHV, advise us to employ these gases as eco-friendly fuels.

3.4.3. Bio-oil fraction.

In the **Fig. 6** it is represented the non-aromatic and aromatic organic compounds present in the obtained bio-oils by conventional and flash pyrolysis. The bio-oils chromatograms are collected in the **Appendix B of the supplementary material document**. Conventional pyrolysis bio-oils were composed of a little fraction of non-aromatic organic compounds (up to 8.35% for CSS-P)

and aromatic organic compounds without benzene rings (up to 17.62 % for CSL-P) whose most representative compounds were acetoxymethyl furaldehyde with a 10.1 % for CSL-P and methyl furanone with a 5.5 % for CSS-P. The greater fraction of this conventional bio-oils were formed by aromatic organic compounds with one benzene ring (75.22 % and 77.13 % for CSL-P and CSS-P, respectively) where phenol and some of their compounds had higher percentages (higher than 55 %). The above ones could be used to produce solvents [2,58]. Dihydrobenzofuran (14.6% for CSL-P) and methoxyethenylphenol (11.49 % for CSS-P) were the organic compounds with higher percentage in these bio-oils. The majority of those organic compounds originated by conventional pyrolysis of CS were formed by oxygenated compounds that decreased the HHV of the bio-oils and increased their acidity [58]. The presence of oxygenated substances indicated a lower viscosity of the bio-oil, which will reduce the cost of the design of a possible application; bio-oils with high viscosity produce poor flow characteristics and combustion properties, for example produce jams for the most fuel injectors [4,57,59].

There were many differences in the bio-oils composition of the flash and conventional pyrolysis. The flash pyrolysis bio-oils were formed mainly by polycyclic aromatic hydrocarbons (PAHs) (up to 98% in CSS-850F) with low percentages in simple organic compounds which were the main compounds in the conventional pyrolysis bio-oils composition, (**Fig. 6**).

Flash pyrolysis bio-oils were made up of PAHs, mainly from 2 to 4 benzene rings (up to 98% for CSS-850F). Aromatic organic compounds and their derivate of naphthalene and fluorene (HAPs with 2 benzene rings), phenanthrene, anthracene and fluotanthene (HAPs with 3 benzene rings), chrysene, pyrene and triphenylene (HAPs with 4 benzene rings) were presented in flash pyrolysis bio-oils of CS.

The flash pyrolysis temperature had an important influence on bio-oils composition, **Fig. 6.** At higher pyrolysis temperature values (850ºC), heavier PAHs were found. This phenomenon was studied by Williams and Nugranad [60]. These authors concluded that this behaviour was common in biomass that generate high amounts of ash which influence in the decomposition of the material, encouraging greater production of PAHs as the temperature rises. The PAHs of the flash pyrolysis bio-oils from CS were originated by side reactions which precursors were phenolic compounds [56].

The different experimental parameters of the pyrolysis process implied that bio-oils composition were different. Each pyrolysis process causes different types of reactions to each CS material [61]. Some of the reactions cited in the scientific associated with this type of process can be the depolymerization, dehydration, hydrogenation, decarbonylation or polycondensation [62].

Bio-oils for CSL-850F and CSS-850F had similar quantities of anthracene and their derivatives (17.7% *vs* 16.6%). However, there were many differences in the following compounds and their derivatives: phenanthrene (18.7% *vs* 26.1%), fluorene (17.2% *vs* 11.2%) and fluoranthene (11.7% *vs* 25.7%). These bio-oils had appreciable quantities of benzopyrene, HAPs with 5 benzene rings, 1.9% in CSL-850F *vs* 3.7% in CSS-850F.

PAHs can be used by the pharmaceutical industry or to produce plastics, explosives, etc. [2,58]. Non-aromatic and aromatic organic compounds without benzene rings were originated by the cellulose and hemicellulose breakdown. Nevertheless, the great majority of the aromatic organic compounds from the conventional and flash pyrolysis had their origin in lignin. In the case of herbaceous biomass, the lignin was composed of 3 monomers: coniferyl alcohol, coumaryl alcohol and synapyl alcohol [25]. The hemicellulose, like lignin, has a heterogeneous composition [58,62]. In the work of Shurong et al [52], it is highlighted that the hemicellulose of herbaceous species is largely composed of arabinoglucuronoxylan polysaccharides; fact that implies that bio-oils have lower degrees of acidity with respect to other bio-oils obtained from other biomass sources [58].

Table 4 shows the bio-oils ultimate analysis and high heating value (HHV). These results were in line with the chromatographic analysis. The C content increased in the flash pyrolysis and with the temperature until achieve a value of 86.67% for CSS-850F. The maximum N values were associated with CSL-750F (possibly due to a large amount of nitrogenous organic compounds [50]). In general, the bio-oils S content was low (0.10 %) with the exception of CSL-P (0.41%). The HHV linked to bio-oils flash pyrolysis were greater (up to 35.52 MJ/kg). Higher temperatures were linked with higher HHV values. Finally, the bio-oils from the CS stems showed higher HHV values than the bio-oils than the CS leaves. The maximum value was found for CSS-850F (35.52 MJ/kg). These values were greater than the results for the bio-oils obtained by flash pyrolysis of

Chlorella vulgaris investigated by Wang et al [63] (HHV= 24.57 MJ/kg) and they were in line with the HHV conventional pyrolysis values [2,4].

3.4.4. Bio-char fraction.

Table 5 presents both the ultimate analysis and HHV of the different bio-char products obtained during flash and conventional pyrolysis. The highest carbon content was observed for CSS-P (85.69%) and, consequently, this value was related to a higher HHV (29.12 MJ/kg). Also, for flash pyrolysis, higher temperature values (850ºC) produced higher C contents in the bio-chars regardless of the part of the biomass. As the bio-chars nitrogen content is corned, values (1.09% - 2.17%) were similar to coal [34] but lower than other biomass [64,65].

The HHV of the bio-chars from CSL (up to 23.81 MJ/kg) were slightly higher than lignite coal (up to 20 MJ/kg) while bio-chars from CSS presented a HHV (up to 29.12 MJ/kg) in the order of bituminous coals [34]. Bio-chars HHV values were over their original biomass values (CSS 19.23 MJ/kg and CSL 18.89 MJ/kg). The bio-chars chemical composition and HHV values were similar to those published for the bio-chars from other biomass obtained by conventional and flash pyrolysis [2,4]. In consequence, bio-chars from both flash and conventional pyrolysis were suitable as fuels due to their high HHV and could also be used as precursors of carbonaceous adsorbent materials because they high carbon content (from 68.78 to 85.69%).

3.5. Scanning electron microscope (SEM).

The CSS and CSL biomass and bio-chars morphological analysis were performed by SEM –EDX. The fibrous vegetable nature of the CSS and CSL biomass is made by alkaline and alkaline earth compounds (like potassium, calcium or magnesium) as can be seen in the sub-sections A and B within the **Appendix C** of the supplementary material document**.** The fibrous nature of CS as well as the presence of Si compounds in this grass have been already reported in literature [6,11,36]. The bio-chars SEM images (Appendix C)**,** showed that they preserved the fibrous structure of the CSS and CSL biomass after the thermal pyrolysis processes at 750 and 850°C. These materials were composed of alkaline and alkaline earth compounds (**section c-f in Appendix C)**, with Si structures that were often cut down (**section b Appendix C**). A plastic phase with devolatization bubbles (some of them have already exploited) was observed in CSV-750F bio-char (**section c**

Appendix C). The vacuoles or bubbles were formed during the pyrolysis process as consequence of volatile matter released into the gas stream. Higher pyrolysis temperatures (850ºC) developed bio-chars with smaller particles due to a higher thermal degradation of CSS and CSL biomass (**section d Appendix C**).

4.- CONCLUSIONS.

In this research and for the first time, a systematic study of the invasive species *Cortaderia selloana* (leaves and stems) as a possible energy source was carried out employing different pyrolysis technologies (conventional and flash). This research showed that it is possible to transform this herbaceous plant, which is an environmental problem, into biofuels (bio-char, bio-oil, and gas). The chemical analysis of the CSL and CSS biomass showed differences in the N content (1.6% and 0.6% respectively). Also, the CSL ash content was higher than CSS values (7.5% *vs* 2.5%). TGA showed mass losses related to moisture, hemicellulose, cellulose and lignin in the same sense that kinetics concluded that CSL had lower E_a values than CSS. The gas part was the main for all the biomass and pyrolysis processes. Together with it, and supporting by their high HHV (17.18 MJ/kg), these gases would be suitable as good eco-friendly fuels. Regarding the rest of the fractions, the largest oil part was achieved for CSS-P (33.58%). Bio-oils composition was different for the different pyrolysis techniques. For its part, chars obtained, which could be successfully used as fuels and carbonaceous adsorbent materials, were higher for CSL-P (26.74%).

REFERENCES

[1] R.E. Guedes, A.S. Luna, A.R. Torres, Operating parameters for bio-oil production in biomass pyrolysis: A review, J. Anal. Appl. Pyrolysis. 129 (2018) 134–149. https://doi.org/https://doi.org/10.1016/j.jaap.2017.11.019.

[2] W. Saadi, S. Rodríguez-Sánchez, B. Ruiz, S. Souissi-Najar, A. Ouederni, E. Fuente, Pyrolysis technologies for pomegranate (Punica granatum L.) peel wastes. Prospects in the bioenergy sector, Renew. Energy. 136 (2019) 373–382. https://doi.org/https://doi.org/10.1016/j.renene.2019.01.017.

[3] G. Ferla, P. Caputo, N. Colaninno, E. Morello, Urban greenery management and energy planning: A GIS-based potential evaluation of pruning by-products for energy application for the city of Milan, Renew. Energy. 160 (2020) 185–195. https://doi.org/10.1016/j.renene.2020.06.105.

[4] V. Dhyani, T. Bhaskar, A comprehensive review on the pyrolysis of lignocellulosic biomass, Renew. Energy. 129 (2018) 695–716. https://doi.org/https://doi.org/10.1016/j.renene.2017.04.035.

[5] E. Rokni, X. Ren, A. Panahi, Y.A. Levendis, Emissions of SO2, NOx, CO2, and HCl from Co-firing of coals with raw and torrefied biomass fuels, Fuel. 211 (2018) 363–374. https://doi.org/10.1016/j.fuel.2017.09.049.

[6] Z. Jia, Z. Li, T. Ni, S. Li, Adsorption of low-cost absorption materials based on biomass (Cortaderia selloana flower spikes) for dye removal: Kinetics, isotherms and thermodynamic studies, J. Mol. Liq. 229 (2017) 285–292. https://doi.org/10.1016/j.molliq.2016.12.059.

[7] S. Tarabon, R. Bertrand, C. Lavoie, T. Vigouroux, F. Isselin-Nondedeu, The effects of climate warming and urbanised areas on the future distribution of Cortaderia selloana, pampas grass, in France, Weed Res. 58 (2018) 413–423. https://doi.org/10.1111/wre.12330.

[8] J. Fagúndez, M. Lema, A competition experiment of an invasive alien grass and two native species: are functionally similar species better competitors?, Biol. Invasions. 21 (2019) 3619–3631. https://doi.org/10.1007/s10530-019-02073-y.

[9] R. Domènech, M. Vilà, Cortaderia selloana invasion across a Mediterranean coastal strip, Acta Oecologica. 32 (2007) 255–261. https://doi.org/https://doi.org/10.1016/j.actao.2007.05.006.

[10] D. Pardo-Primoy, J. Fagúndez, Assessment of the distribution and recent spread of the invasive grass Cortaderia selloana in Industrial Sites in Galicia, NW Spain, Flora. 259 (2019) 151465. https://doi.org/10.1016/J.FLORA.2019.151465.

[11] M.F. Honaine, N.L. Borrelli, M. Osterrieth, L. del Rio, Leaf and culm silicification of Pampas grass (*Cortaderia selloana*) developed on different soils from Pampean region, Argentina, Aust. J. Bot. 65 (2017) 1–10.

[12] A.L.P. Dresseno, A. Guido, V. Balogianni, G.E. Overbeck, Negative effects of an invasive grass, but not of native grasses, on plant species richness along a cover gradient, Austral Ecol. 43 (2018) 949–954. https://doi.org/10.1111/aec.12644.

[13] A. Jordá-Vilaplana, A. Carbonell-Verdú, M.D. Samper, A. Pop, D. Garcia-Sanoguera, Development and characterization of a new natural fiber reinforced thermoplastic (NFRP) with Cortaderia selloana (Pampa grass) short fibers, Compos. Sci. Technol. 145 (2017) 1–9. https://doi.org/10.1016/J.COMPSCITECH.2017.03.036.

[14] A.M. Smith, C. Whittaker, I. Shield, A.B. Ross, The potential for production of high quality bio-coal from early harvested Miscanthus by hydrothermal carbonisation, Fuel. 220 (2018) 546–557. https://doi.org/10.1016/j.fuel.2018.01.143.

[15] S. Shilpi, D. Lamb, N. Bolan, B. Seshadri, G. Choppala, R. Naidu, Waste to watt: Anaerobic digestion of wastewater irrigated biomass for energy and fertiliser production, J. Environ. Manage. 239 (2019) 73–83. https://doi.org/10.1016/j.jenvman.2019.02.122.

[16] S. Wan, V.M.T. Truong-Trieu, T. Ward, J.K. Whalen, I. Altosaar, Advances in the use of genetically modified plant biomass for biodiesel generation, Biofuels, Bioprod. Biorefining. 11 (2017) 749–764. https://doi.org/10.1002/bbb.1777.

[17] M. Afsharpour, E. Khomand, Synthesis of bio-inspired porous silicon carbides using Cortaderia selloana and Equisetum arvense grasses as remarkable sulfur adsorbents, Int. J. Environ. Sci. Technol. (2018). https://doi.org/10.1007/s13762-018-1679-x.

[18] N. Mechi, I. Ben Khemis, G.L. Dotto, D. Franco, L. Sellaoui, A. Ben Lamine, Investigation of the adsorption mechanism of methylene blue (MB) on Cortaderia selloana flower spikes

(FSs) and on Cortaderia selloana flower spikes derived carbon fibers (CFs), J. Mol. Liq. 280 (2019) 268–273. https://doi.org/https://doi.org/10.1016/j.molliq.2019.02.024.
[19] Y. Shi, X. Liang, Novel carbon microtube based solid acid from pampas grass stick for biodiesel synthesis from waste oils, J. Saudi Chem. Soc. 23 (2019) 515–524. https://doi.org/https://doi.org/10.1016/j.jscs.2018.09.004.
[20] M. Gogoi, K. Konwar, N. Bhuyan, R.C. Borah, A.C. Kalita, H.P. Nath, N. Saikia, Assessments of pyrolysis kinetics and mechanisms of biomass residues using thermogravimetry, Bioresour. Technol. Reports. 4 (2018) 40–49. https://doi.org/https://doi.org/10.1016/j.biteb.2018.08.016.
[21] B. Saletnik, G. Zagula, M. Bajcar, M. Czernicka, C. Puchalski, Biochar and biomass ash as a soil ameliorant: The effect on selected soil properties and yield of Giant Miscanthus (Miscanthus x giganteus), Energies. 11 (2018) 2535.
[22] V. Chaloupková, T. Ivanova, O. Ekrt, A. Kabutey, D. Herák, Determination of particle size and distribution through image-based macroscopic analysis of the structure of biomass briquettes, Energies. 11 (2018) 331.
[23] D. Castello, B. Rolli, A. Kruse, L. Fiori, Supercritical water gasification of biomass in a ceramic reactor: Long-time batch experiments, Energies. 10 (2017) 1734.
[24] Z. Kaczor, Z. Buliński, S. Werle, Modelling approaches to waste biomass pyrolysis: a review, Renew. Energy. 159 (2020) 427–443. https://doi.org/10.1016/j.renene.2020.05.110.
[25] S. Hameed, A. Sharma, V. Pareek, H. Wu, Y. Yu, A review on biomass pyrolysis models: Kinetic, network and mechanistic models, Biomass and Bioenergy. 123 (2019) 104–122. https://doi.org/https://doi.org/10.1016/j.biombioe.2019.02.008.
[26] A. Patel, B. Agrawal, B.R. Rawal, Pyrolysis of biomass for efficient extraction of biofuel, Energy Sources, Part A Recover. Util. Environ. Eff. 42 (2020) 1649–1661.
[27] P.L. Dulong, A.T. Petit, Recherches sur la mesure des temperatures et sur les lois de la communication de la chaleur, 1st ed., De l'Imprimerie royale, Paris, 1818.
[28] D. Beckman, Techno-economic assessment of selected biomass liquefaction processes, Valtion teknillinen tutkimuskeskus, Espoo; Helsinki, 1990.
[29] D. Lv, M. Xu, X. Liu, Z. Zhan, Z. Li, H. Yao, Effect of cellulose, lignin, alkali and alkaline earth metallic species on biomass pyrolysis and gasification, Fuel Process. Technol. 91 (2010) 903–909. https://doi.org/https://doi.org/10.1016/j.fuproc.2009.09.014.
[30] R.K. Agrawal, M.S. Sivasubramanian, Integral approximations for nonisothermal kinetics, AIChE J. 33 (1987) 1212–1214. https://doi.org/10.1002/aic.690330716.
[31] B. Ruiz, N. Ferrera-Lorenzo, E. Fuente, Valorisation of lignocellulosic wastes from the candied chestnut industry. Sustainable activated carbons for environmental applications, J. Environ. Chem. Eng. 5 (2017) 1504–1515. https://doi.org/10.1016/J.JECE.2017.02.028.
[32] S. Paniagua, A.I. García-Pérez, L.F. Calvo, Biofuel consisting of wheat straw–poplar wood blends: thermogravimetric studies and combustion characteristic indexes estimation, Biomass Convers. Biorefinery. 9 (2019) 433–443. https://doi.org/10.1007/s13399-018-0351-5.
[33] B. Biswas, N. Pandey, Y. Bisht, R. Singh, J. Kumar, T. Bhaskar, Pyrolysis of agricultural biomass residues: Comparative study of corn cob, wheat straw, rice straw and rice husk, Bioresour. Technol. 237 (2017) 57–63. https://doi.org/https://doi.org/10.1016/j.biortech.2017.02.046.
[34] J.A. Pajares, M.A. DiezDíez, COAL AND COKE, in: P. Worsfold, A. Townshend, C. Poole (Eds.), Encycl. Anal. Sci. (Second Ed., Second Edi, Elsevier, Oxford, 2005: pp. 182–197. https://doi.org/https://doi.org/10.1016/B0-12-369397-7/00099-6.
[35] M. Osterrieth, N. Borrelli, M.F. Alvarez, M. Fernández Honaine, Silica biogeochemical cycle in temperate ecosystems of the Pampean Plain, Argentina, J. South Am. Earth Sci. 63 (2015) 172–179. https://doi.org/https://doi.org/10.1016/j.jsames.2015.07.011.
[36] F.C. Lanning, L.N. Eleuterius, Silica Deposition in Some C3 and C4 Species of Grasses, Sedges and Composites in the USA, Ann. Bot. 64 (1989) 395–410. https://doi.org/10.1093/oxfordjournals.aob.a087858.
[37] J. Raven, THE TRANSPORT AND FUNCTION OF SILICON IN PLANTS, Biol. Rev. 58 (1983) 179–207. https://doi.org/10.1111/j.1469-185X.1983.tb00385.x.
[38] Y. Yang, X. Lu, Q. Wang, Investigation on the co-combustion of low calorific oil shale and its semi-coke by using thermogravimetric analysis, Energy Convers. Manag. 136 (2017) 99–107. https://doi.org/10.1016/J.ENCONMAN.2017.01.006.
[39] H.H. Sait, A. Hussain, A.A. Salema, F.N. Ani, Pyrolysis and combustion kinetics of date

palm biomass using thermogravimetric analysis, Bioresour. Technol. 118 (2012) 382–389. https://doi.org/10.1016/J.BIORTECH.2012.04.081.
[40] H. Haykırı-Açma, Combustion characteristics of different biomass materials, Energy Convers. Manag. 44 (2003) 155–162.
[41] S. Gaur, T.B. Reed, Thermal Data for Natural and Synthetic Fuels, Marcel Deeker, in: Inc. New York, NY, USA, 1998: pp. 239–241.
[42] M.T. Moreira, I. Noya, G. Feijoo, The prospective use of biochar as adsorption matrix – A review from a lifecycle perspective, Bioresour. Technol. 246 (2017) 135–141. https://doi.org/10.1016/j.biortech.2017.08.041.
[43] Y. Wang, H. Tan, X. Wang, W. Du, H. Mikulčić, N. Duić, Study on extracting available salt from straw/woody biomass ashes and predicting its slagging/fouling tendency, J. Clean. Prod. 155 (2017) 164–171. https://doi.org/10.1016/j.jclepro.2016.08.102.
[44] Y. Niu, H. Tan, S. Hui, Ash-related issues during biomass combustion: Alkali-induced slagging, silicate melt-induced slagging (ash fusion), agglomeration, corrosion, ash utilization, and related countermeasures, Prog. Energy Combust. Sci. 52 (2016) 1–61. https://doi.org/10.1016/j.pecs.2015.09.003.
[45] S. Tang, Y. Tang, C. Zheng, Z. Zhang, Alkali metal-driven release behaviors of volatiles during sewage sludge pyrolysis, J. Clean. Prod. 203 (2018) 860–872. https://doi.org/10.1016/j.jclepro.2018.08.312.
[46] A. Monti, N. Di Virgilio, G. Venturi, Mineral composition and ash content of six major energy crops, Biomass and Bioenergy. 32 (2008) 216–223. https://doi.org/10.1016/j.biombioe.2007.09.012.
[47] G. Zając, J. Szyszlak-Bargłowicz, W. Gołębiowski, M. Szczepanik, Chemical Characteristics of Biomass Ashes, Energies. 11 (2018) 2885. https://doi.org/10.3390/en11112885.
[48] T. Rehren, A review of factors affecting the composition of early Egyptian glasses and faience: alkali and alkali earth oxides, J. Archaeol. Sci. 35 (2008) 1345–1354. https://doi.org/10.1016/J.JAS.2007.09.005.
[49] M. Imtiaz, M.S. Rizwan, M.A. Mushtaq, M. Ashraf, S.M. Shahzad, B. Yousaf, D.A. Saeed, M. Rizwan, M.A. Nawaz, S. Mehmood, S. Tu, Silicon occurrence, uptake, transport and mechanisms of heavy metals, minerals and salinity enhanced tolerance in plants with future prospects: A review, J. Environ. Manage. 183 (2016) 521–529. https://doi.org/https://doi.org/10.1016/j.jenvman.2016.09.009.
[50] J. Rumble, ed., CRC handbook of chemistry and physics : a ready-reference book of chemical and physical data., 100th ed., CRC Press, Boca Raton, 2019.
[51] L. Wang, G. Skjevrak, Ø. Skreiberg, H. Wu, H.K. Nielsen, J.E. Hustad, Investigation on Ash Slagging Characteristics during Combustion of Biomass Pellets and Effect of Additives, Energy and Fuels. 32 (2018) 4442–4452. https://doi.org/10.1021/acs.energyfuels.7b03173.
[52] W. Shurong, D. Gongxin, Y. Haiping, L. Zhongyang, Lignocellulosic biomass pyrolysis mechanism: A state-of-the-art review, Prog. Energy Combust. Sci. 62 (2017) 33–86. https://doi.org/10.1016/j.pecs.2017.05.004.
[53] S. Paniagua, L. Escudero, R.N. Coimbra, C. Escapa, M. Otero, L.F. Calvo, Effect of Applying Organic Amendments on the Pyrolytic Behavior of a Poplar Energy Crop, Waste and Biomass Valorization. 9 (2018) 1435–1449. https://doi.org/10.1007/s12649-017-9885-1.
[54] T. Sonobe, N. Worasuwannarak, Kinetic analyses of biomass pyrolysis using the distributed activation energy model, Fuel. 87 (2008) 414–421. https://doi.org/http://dx.doi.org/10.1016/j.fuel.2007.05.004.
[55] S. Sun, H. Tian, Y. Zhao, R. Sun, H. Zhou, Experimental and numerical study of biomass flash pyrolysis in an entrained flow reactor, Bioresour. Technol. 101 (2010) 3678–3684. https://doi.org/https://doi.org/10.1016/j.biortech.2009.12.092.
[56] K. Maliutina, A. Tahmasebi, J. Yu, S.N. Saltykov, Comparative study on flash pyrolysis characteristics of microalgal and lignocellulosic biomass in entrained-flow reactor, Energy Convers. Manag. 151 (2017) 426–438. https://doi.org/https://doi.org/10.1016/j.enconman.2017.09.013.
[57] T. Kan, V. Strezov, T.J. Evans, Lignocellulosic biomass pyrolysis: A review of product properties and effects of pyrolysis parameters, Renew. Sustain. Energy Rev. 57 (2016) 1126–1140. https://doi.org/http://dx.doi.org/10.1016/j.rser.2015.12.185.
[58] O.D. Mante, S.P. Babu, T.E. Amidon, A comprehensive study on relating cell-wall

components of lignocellulosic biomass to oxygenated species formed during pyrolysis, J. Anal. Appl. Pyrolysis. 108 (2014) 56–67. https://doi.org/https://doi.org/10.1016/j.jaap.2014.05.016.
[59] M. Balat, M. Balat, E. Kırtay, H. Balat, Main routes for the thermo-conversion of biomass into fuels and chemicals. Part 1: Pyrolysis systems, Energy Convers. Manag. 50 (2009) 3147–3157. https://doi.org/https://doi.org/10.1016/j.enconman.2009.08.014.
[60] P.T. Williams, N. Nugranad, Comparison of products from the pyrolysis and catalytic pyrolysis of rice husks, Energy. 25 (2000) 493–513. https://doi.org/https://doi.org/10.1016/S0360-5442(00)00009-8.
[61] J.E. White, W.J. Catallo, B.L. Legendre, Biomass pyrolysis kinetics: A comparative critical review with relevant agricultural residue case studies, J. Anal. Appl. Pyrolysis. 91 (2011) 1–33. https://doi.org/http://dx.doi.org/10.1016/j.jaap.2011.01.004.
[62] P. Schroeder, B.P. do Nascimento, G.A. Romeiro, M.K.-K. Figueiredo, M.C. da Cunha Veloso, Chemical and physical analysis of the liquid fractions from soursop seed cake obtained using slow pyrolysis conditions, J. Anal. Appl. Pyrolysis. 124 (2017) 161–174. https://doi.org/https://doi.org/10.1016/j.jaap.2017.02.010.
[63] K. Wang, R.C. Brown, S. Homsy, L. Martinez, S.S. Sidhu, Fast pyrolysis of microalgae remnants in a fluidized bed reactor for bio-oil and biochar production, Bioresour. Technol. 127 (2013) 494–499. https://doi.org/10.1016/j.biortech.2012.08.016.
[64] N. Ferrera-Lorenzo, E. Fuente, I. Suárez-Ruiz, R.R. Gil, B. Ruiz, Pyrolysis characteristics of a macroalgae solid waste generated by the industrial production of Agar–Agar, J. Anal. Appl. Pyrolysis. 105 (2014) 209–216. https://doi.org/10.1016/J.JAAP.2013.11.006.
[65] N. Ferrera-Lorenzo, E. Fuente, J.M. Bermúdez, I. Suárez-Ruiz, B. Ruiz, Conventional and microwave pyrolysis of a macroalgae waste from the Agar–Agar industry. Prospects for bio-fuel production, Bioresour. Technol. 151 (2014) 199–206. https://doi.org/10.1016/J.BIORTECH.2013.10.047.

FIGURE CAPTIONS

Fig.1. a) Pyrolysis set up b) Stick with mechanical device.

Fig.2. ICP-MS analysis for CSS (a) and CSL (b) ashes in dry basis.

Fig.3. TG and DTG profiles for CSS (a) and CSL (b) under three different heating rates.

Fig.4. Yield of gas, bio-oil and bio-char fractions in the different pyrolytic processes

Fig.5. Composition of the gas fraction for the different *Cortaderia selloana* biomass and pyrolysis processes.

Fig.6. Composition of the Bio-oil fraction for the different *Cortaderia selloana* biomass and pyrolysis processes classified by non aromatic and aromatic organic compounds.

Fig.7.CSS biomass SEM-EDX detail of a) Si compounds b) vegetable fibres.

Fig.8. a) SEM of CSL-750F b) SEM-EDX of CSS-850F c) SEM of CSS-750F d) SEM of CSS-P and CSS-850F.

LIST OF ABBREVIATIONS.

COS: Carbonyl sulphide.

CS: *Cortaderia selloana*.

CSL: Biomass related to *Cortaderia selloana* leaves.

CSL-750F: Flash pyrolysis at 750ºC for *Cortaderia selloana* leaves.

CSL-850F: Flash pyrolysis at 850ºC for *Cortaderia selloana* leaves.

CSL-P: Conventional pyrolysis for *Cortaderia selloana* leaves.

CSS: Biomass related to *Cortaderia selloana* stems.

CSS-750F: Flash pyrolysis at 750ºC for *Cortaderia selloana* stems.

CSS-850F: Flash pyrolysis at 850ºC for *Cortaderia selloana* stems.

CSS-P: Conventional pyrolysis for *Cortaderia selloana* stems.

EDX: energy-dispersive X-ray.

FC: Fixed Carbon.

H_2S: Hydrogen sulphide

HHV: Higher heating value.

LHV: Lower heating value.

SEM: Scanning electron microscope.

TCD: Thermal conductivity detector.

VM: Volatile matter.

TGA: Thermogravimetric analysis.

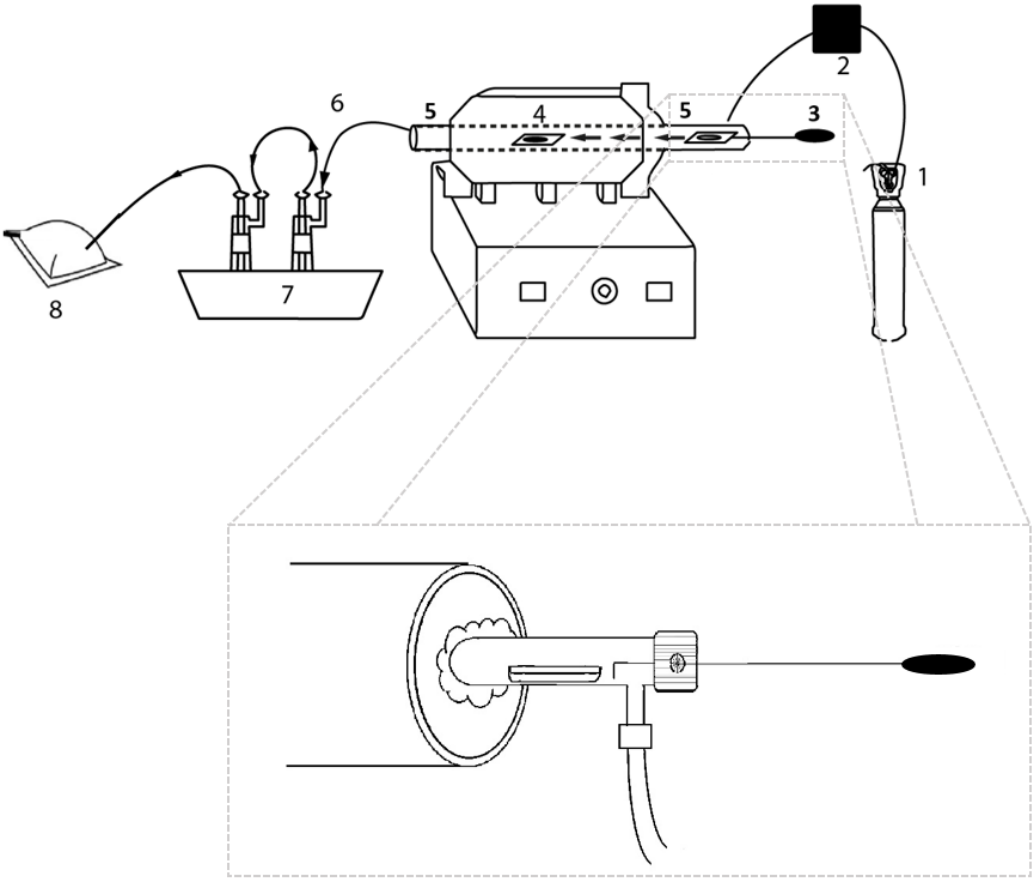

Fig.1. Pyrolysis set up schema. (1) N_2; (2) N_2 mass controller; (3) stick to introduce the sample into the reactor; (4) sample inside the reactor; (5) reactor with a quartz; tube (6) release of volatile compounds after the pyrolysis process; (7) cooler for condensation of bio oils: (8) Tedlar bag for gas collection

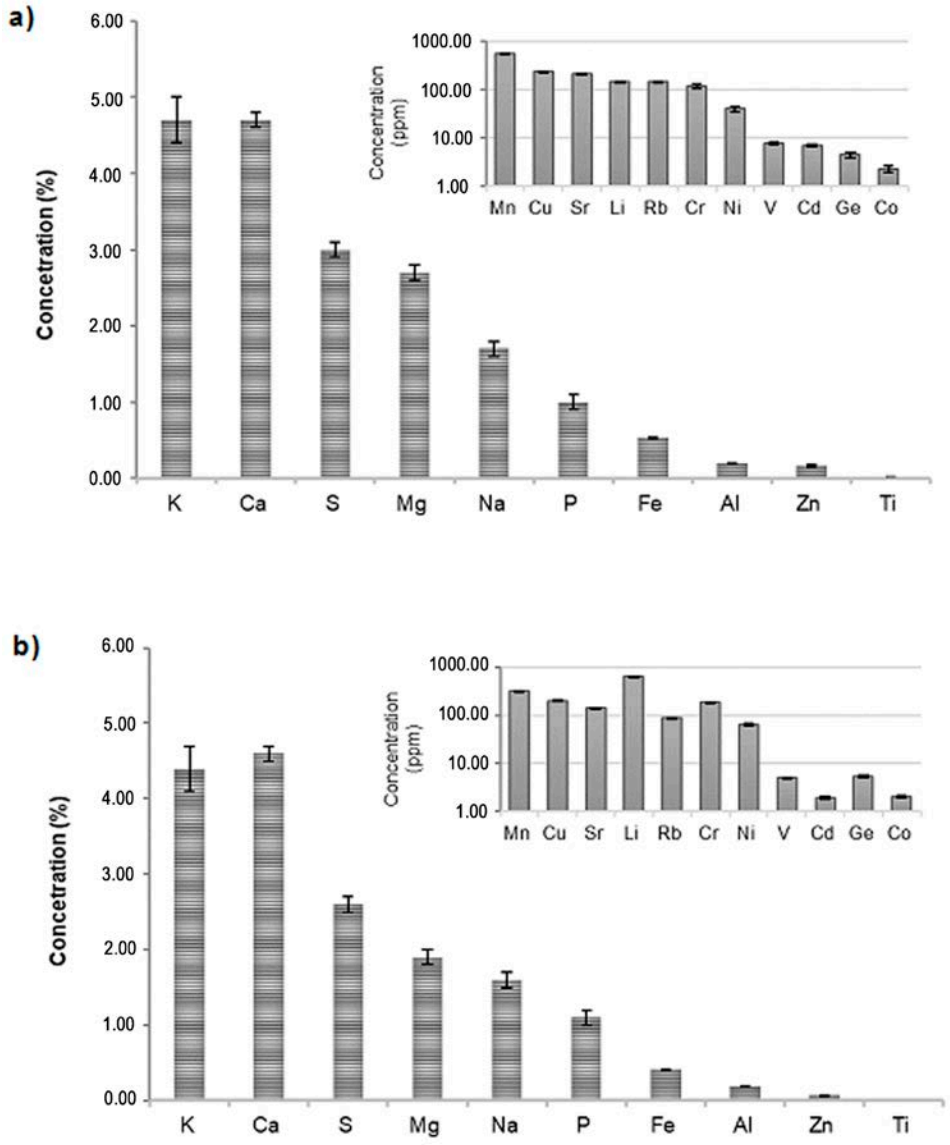

Fig.2. ICP-MS analysis for CSS (a) and CSL (b) ashes in dry basis.

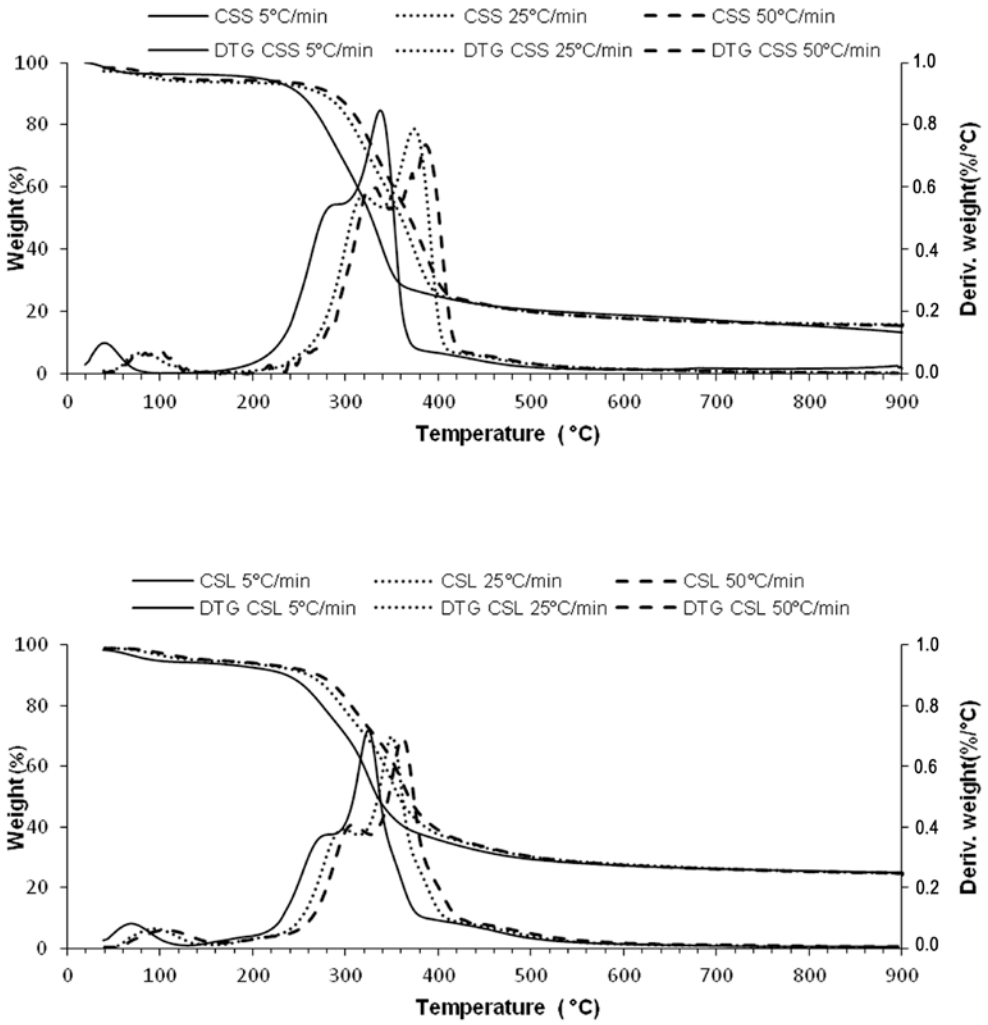

Fig.3. TG and DTG profiles for CSS (a) and CSL (b) under three different heating rates.

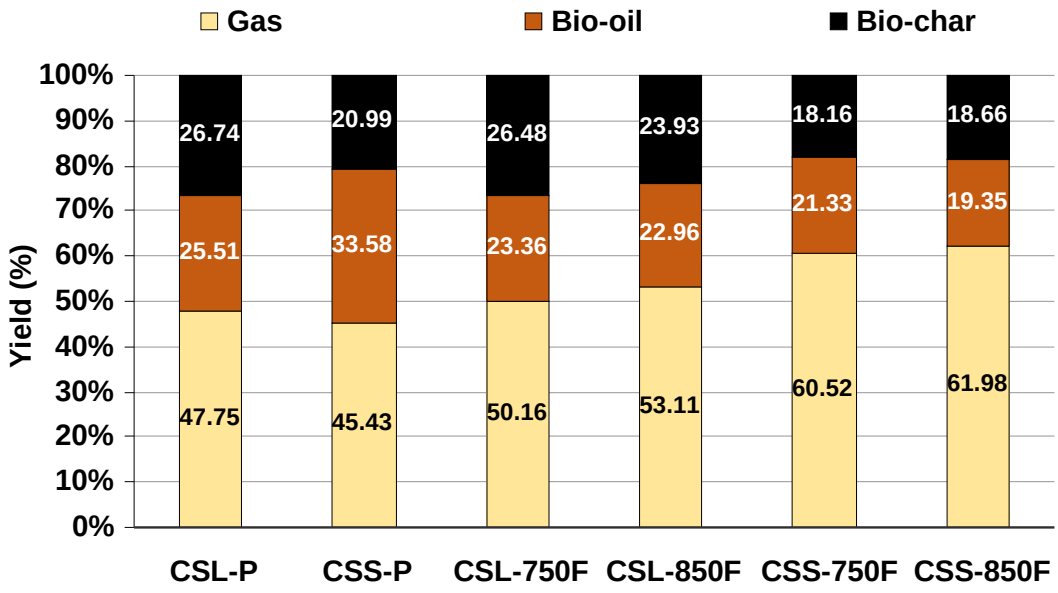

Fig.4. Yield of gas, bio-oil and bio-char fractions in the different pyrolytic processes

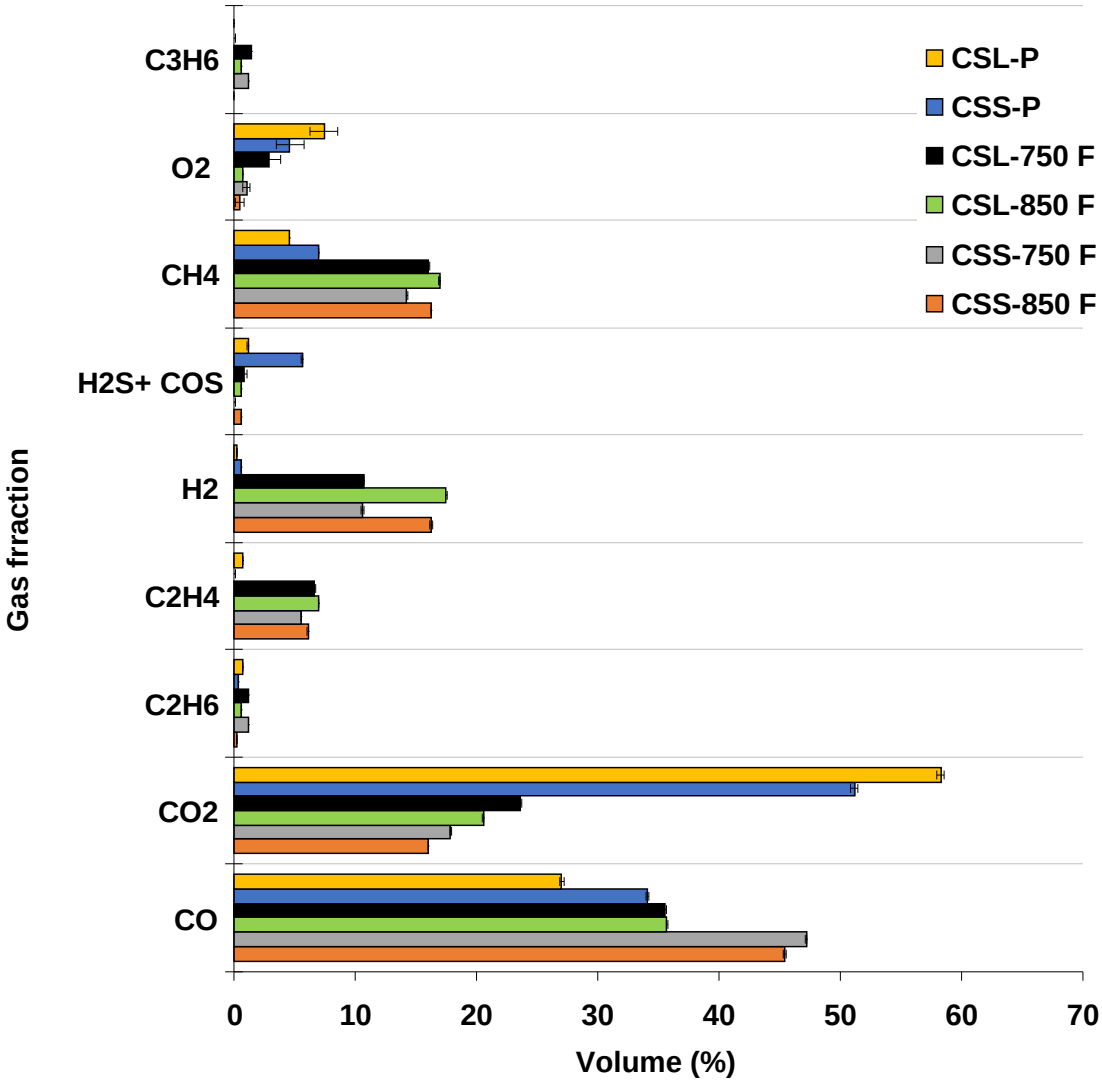

Fig.5. Relative composition of the gas fractions for the different Cortaderia Selloana biomass pyrolysis processes

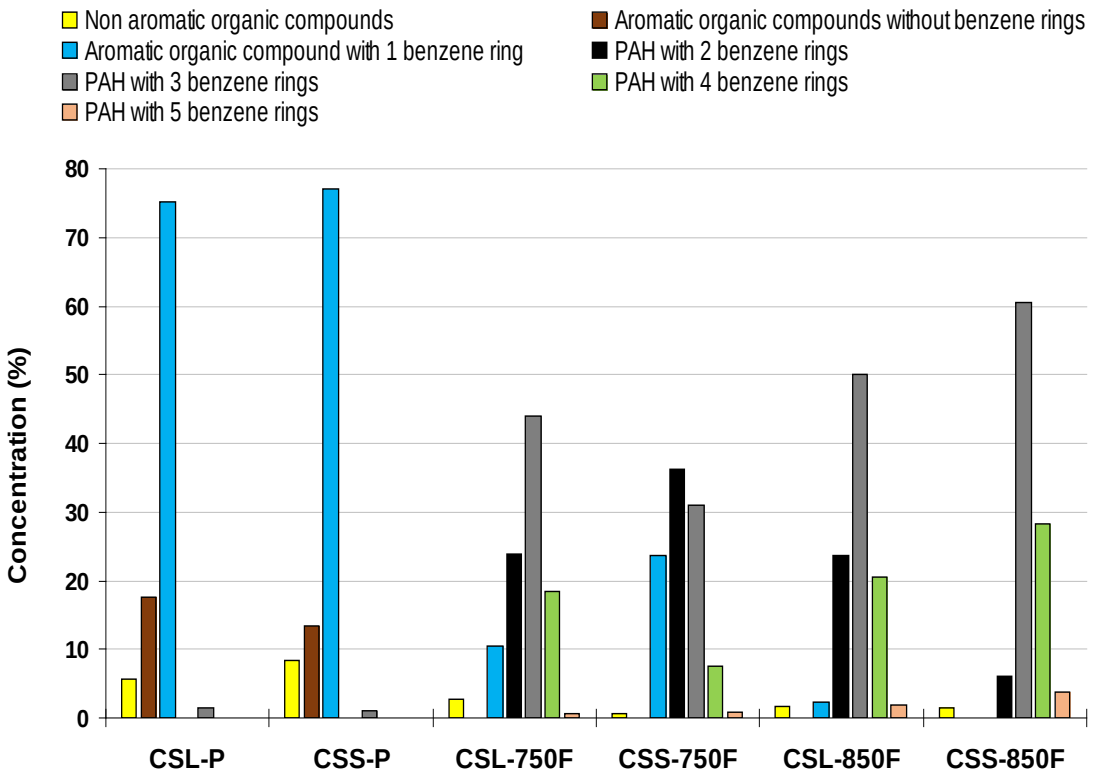

Fig.6. Composition of the Bio-oil fraction for the different *Cortaderia selloana* biomass and pyrolysis processes classified by non aromatic and aromatic organic compounds.

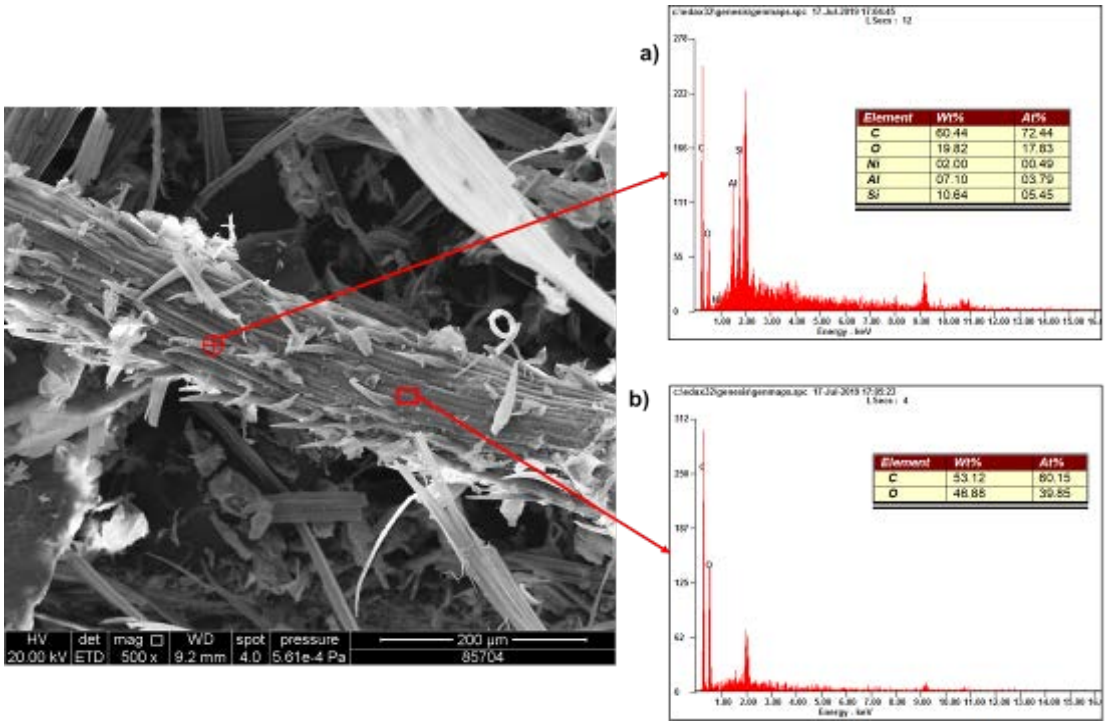

Fig.7. CSS biomass SEM-EDX detail of a) Si compounds b) vegetable fibres.

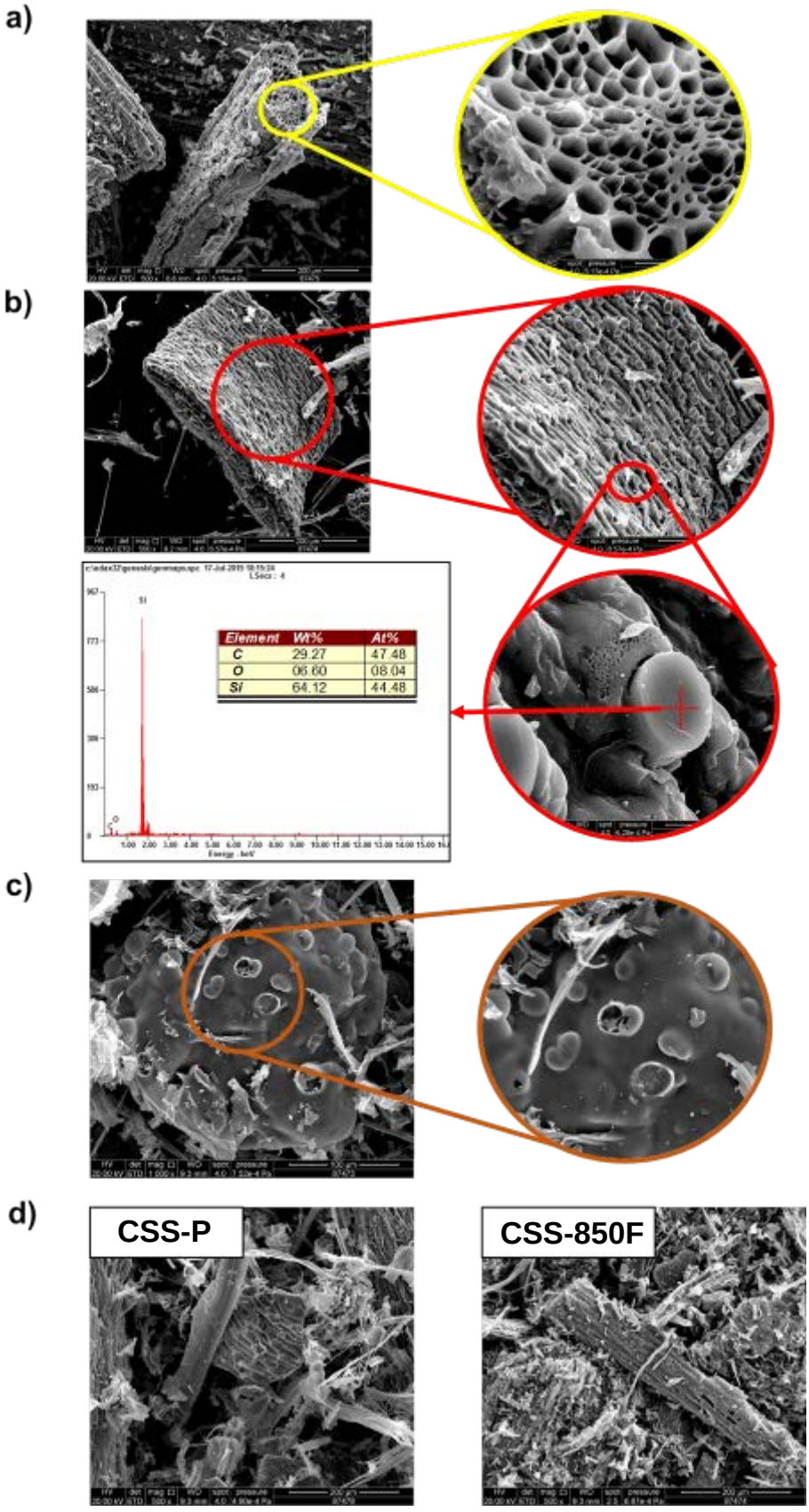

Fig.8. a) SEM of CSL-750F b) SEM-EDX of CSS-850F c) SEM of CSS-750F d) SEM of CSS-P and CSS-850F.

Table 1. Ultimate and proximate analysis and calorific values for pampa grass (CS) biomass.

	Ultimate analysis					Proximate analysis					
	C[a] (%)	H[a] (%)	N[a] (%)	S[a] (%)	O[ab] (%)	Moisture (%)	Ash[a] (%)	VM[a] (%)	FC[ab] (%)	HHV (MJ/kg)	LHV (MJ/kg)
CSS	48.5 ± 0.1	5.9 ± 0.1	0.6 ± 0.1	0.10 ± 0.01	42.5 ± 0.6	6.1 ± 0.4	2.5 ± 0.5	81.9 ± 0.4	9.5 ± 0.5	19.20 ± 0.07	18.00 ± 0.04
CSL	46.7 ± 0.4	5.7 ± 0.1	1.6 ± 0.1	0.20 ± 0.01	38.3 ± 0.1	6.7 ± 0.2	7.5 ± 0.5	74.8 ± 0.3	10.6 ± 0.6	18.90 ± 0.04	17.70 ± 0.06

[a] Dry basis. [b] Determined by difference.

Table 2. *Cortaderia selloana* DTG pyrolysis profiles characteristic parameters and kinetic values.

Biomass	Heating rate (ºC/min)	$T_{range\ (He-Li)}$ (ºC)	DTG_{max} (%/ºC)	T_{DTGmax} (ºC)	E_a (kJ/mol)	k_0 (1/s)	R^2
CSS	5	117.18 – 513.92	0.8460	337.03	222.85	5,13E+16	0,96
CSS	25	189.22 – 582.20	0.7852	374.93	269.02	2,02E+19	0,95
CSS	50	161.82 – 577.09	0.7362	386.73	292.84	5,72E+20	0,94
CSL	5	139.05 – 593.79	0.7192	324.39	164.07	4,43E+11	0,90
CSL	25	166.03 – 598.59	0.6985	349.66	164.83	1,97E+10	0,93
CSL	50	160.98 – 628.26	0.6945	361.46	168.17	1,43E+11	0,91

$T_{range\ (He-Li)}$: temperature range related with the decomposition of hemicellulose, cellulose and lignin.

DTG_{max}: largest value of DTG in the considered process. T_{DTGmax} : temperature associated to DTG_{max}.

E_a: activation energy. K_0: frequency factor. R^2: coefficient of determination.

Table 3. *Cortaderia selloana* high heating value for the gas fractions obtained under the different pyrolysis processes.

Biomass – pyrolysis type	HHV (MJ/kg)
CSS-P	5.77
CSS-750F	15.86
CSS-850F	16.77
CSL-P	4.26
CSL-750F	15.92
CSL-850F	17.18

Table 4. Bio-oils elemental analysis and calorific values.

	Ultimate analysis					HHV (MJ/kg)
	C^{a} (%)	H^{a} (%)	N^{a} (%)	S^{a} (%)	O^{ab} (%)	
CSS-P	52.25	6.34	0.30	0.10	41.01	20.40
CSS-750F	75.28	8.32	3.37	0.10	12.93	33.42
CSS-850F	86.67	5.73	0.89	0.10	6.61	35.52
CSL-P	57.89	6.67	2.68	0.41	32.35	23.65
CSL-750F	79.25	5.96	5.32	0.10	9.37	32.85
CSL-850F	80.49	5.69	4.46	0.10	9.26	33.03

[a] Dry basis. [b] Determined by difference.

Table 5. Chars ultimate analysis, HHV and ashes.

	Ultimate analysis					HHV (MJ/kg)	Ash (%)
	C^a (%)	H^a (%)	N^a (%)	S^a (%)	O^{ab} (%)		
CSS-P	85.69	1.16	1.19	0.21	1.75	29.12	10.00
CSS-750F	81.89	1.53	1.09	0.27	4.49	27.40	10.73
CSS-850F	84.04	1.17	1.18	0.23	3.27	28.28	10.11
CSL-P	71.24	0.96	2.17	0.38	3.78	23.81	21.47
CSL-750F	68.78	1.48	2.13	0.42	5.61	22.74	21.58
CSL-850F	70.15	0.91	2.03	0.43	1.98	23.75	24.50

[a] Dry basis. [b] Determined by difference.

Supporting Information for:

Pyrolysis technology for *Cortaderia selloana* invasive species. Prospects in the biomass energy sector.

Alejandro Pérez[1], Begoña Ruiz[1], Enrique Fuente[1], Luis Fernando Calvo[2*], Sergio Paniagua[2].

[1]Biocarbon and Sustainability Group (B&S), Instituto de Ciencia y Tecnología del Carbono, INCAR-CSIC. Francisco Pintado Fe, 26. 33011 Oviedo, Spain.

[2] University of León, Department of Chemistry and Applied Physics, Chemical Engineering Area, IMARENABIO, Avda. Portugal 41 (24071), León, Spain.

* Corresponding author email: lfcalp@unileon.es

Telephone: +34 987291843

APPENDIX A: Scheme of sample preparation of CSL and CSS biomass.

The separation of CSS and CSL was carried out in the invaded area. Later, a first separation was made to grind and sift biomass and thus obtain an ideal particle size for experimental analyses.

Cortaderia selloana

APPENDIX B: CHROMATOGRAPHIC ANALYSIS COMPLEMENTARY INFORMATION.

Bio-oils chromatograms. X-axis shows the retention time(min) and Y-axis the abundance or absorbance (dimensionless) for each peak.

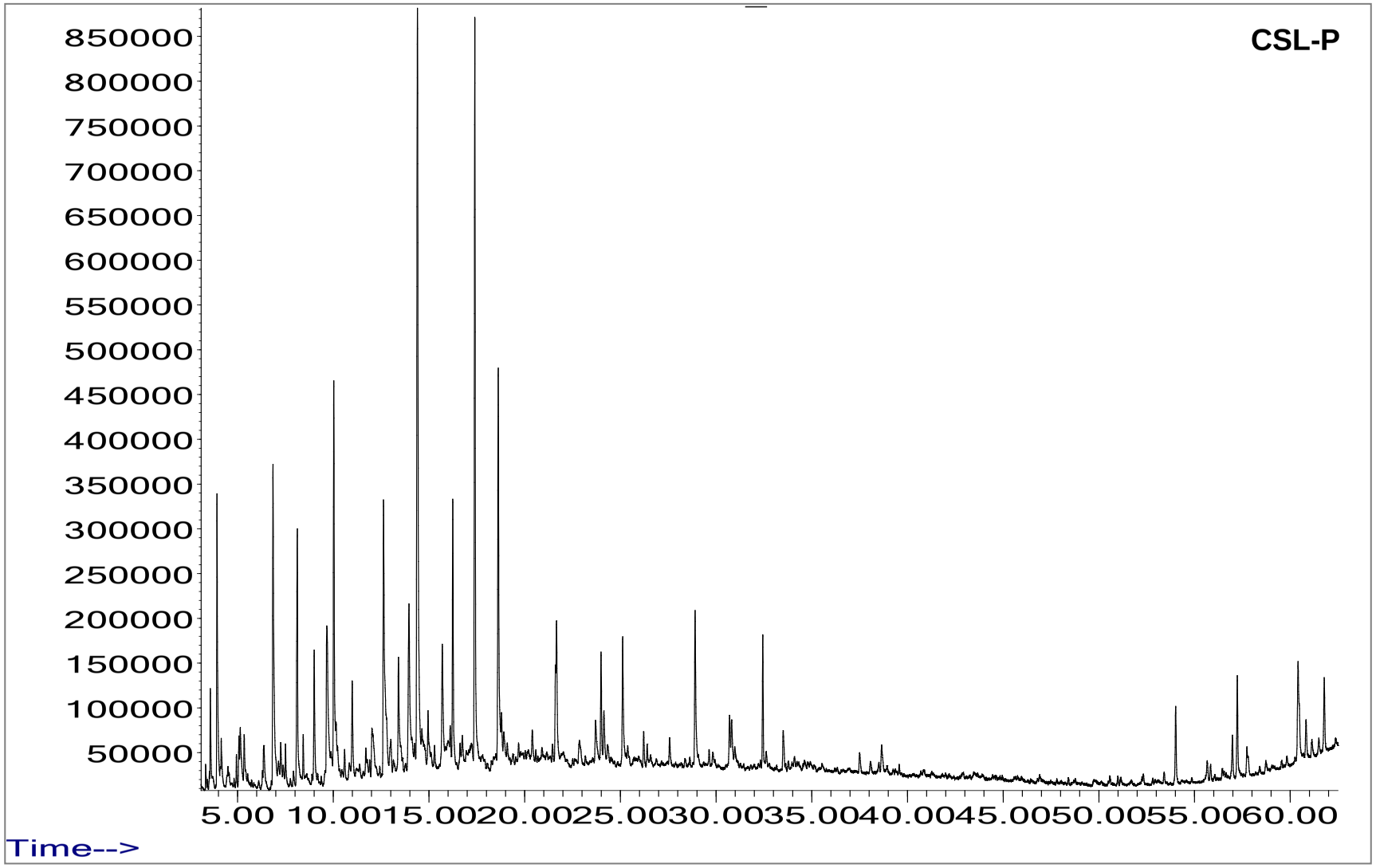

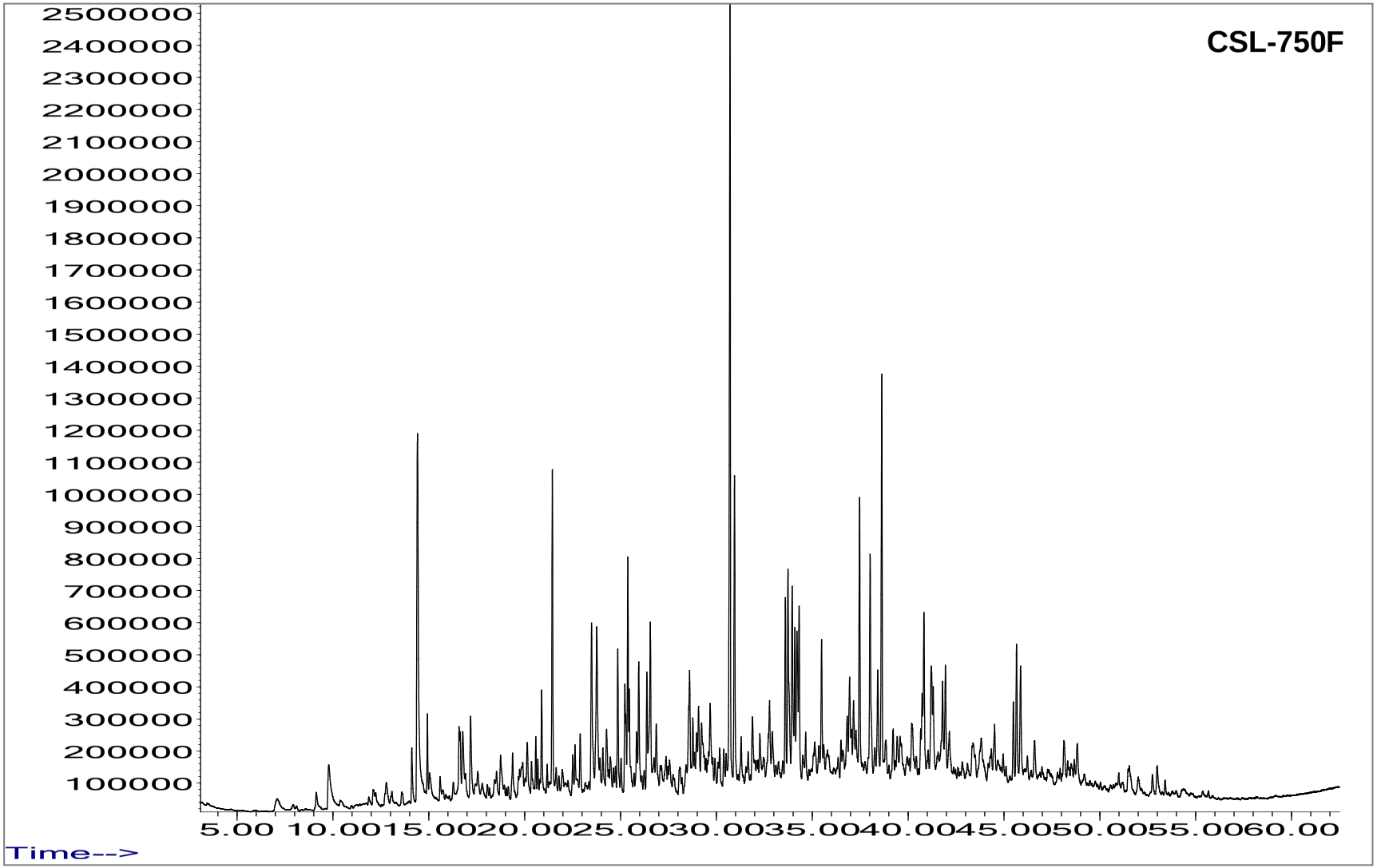
CSL-750F
2500000
2400000
2300000
2200000
2100000
2000000
1900000
1800000
1700000
1600000
1500000
1400000
1300000
1200000
1100000
1000000
900000
800000
700000
600000
500000
400000
300000
200000
100000
5.00 10.00 15.00 20.00 25.00 30.00 35.00 40.00 45.00 50.00 55.00 60.00
Time-->

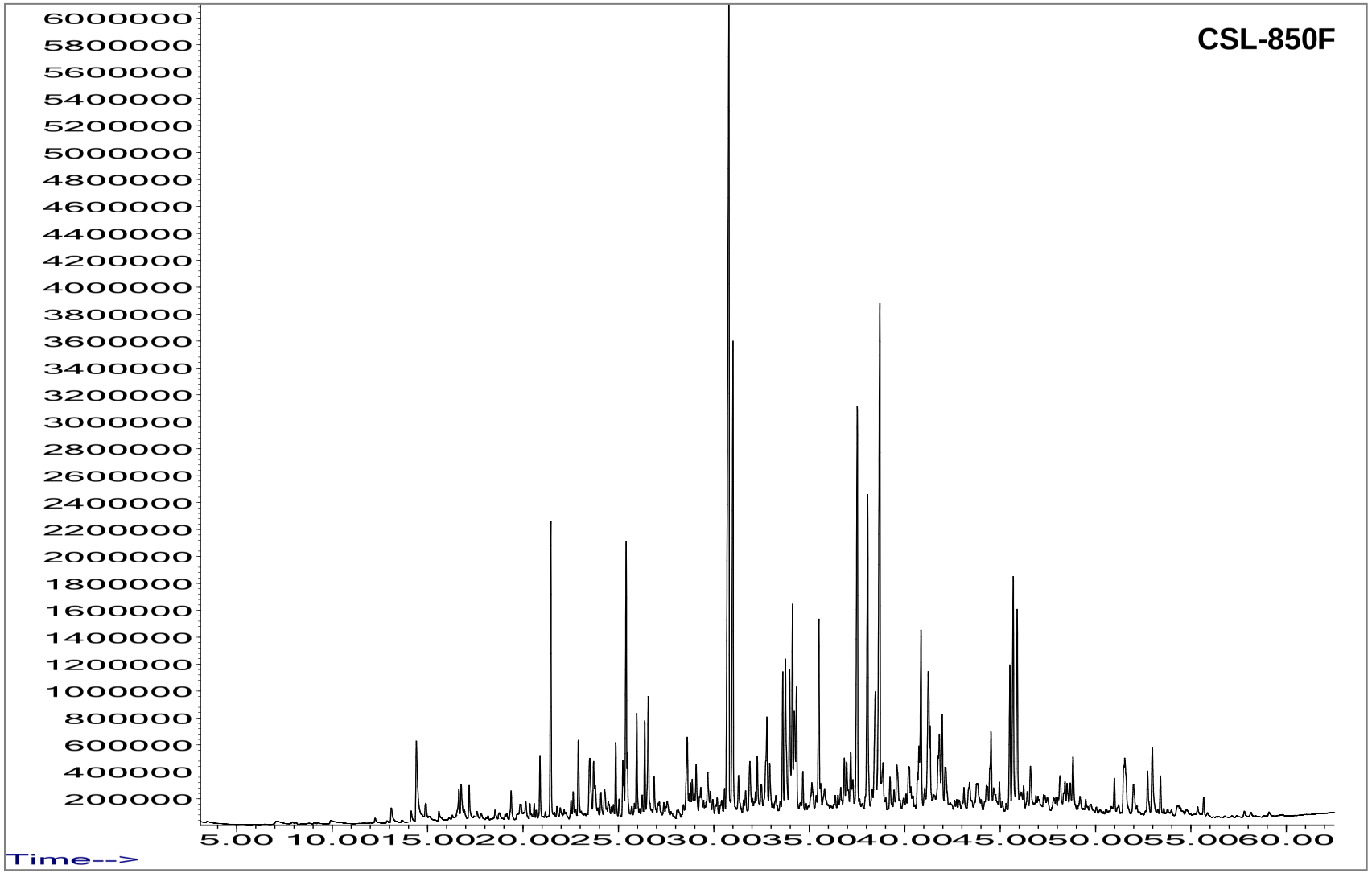
CSL-850F
6000000
5800000
5600000
5400000
5200000
5000000
4800000
4600000
4400000
4200000
4000000
3800000
3600000
3400000
3200000
3000000
2800000
2600000
2400000
2200000
2000000
1800000
1600000
1400000
1200000
1000000
800000
600000
400000
200000
5.00 10.00 15.00 20.00 25.00 30.00 35.00 40.00 45.00 50.00 55.00 60.00
Time-->

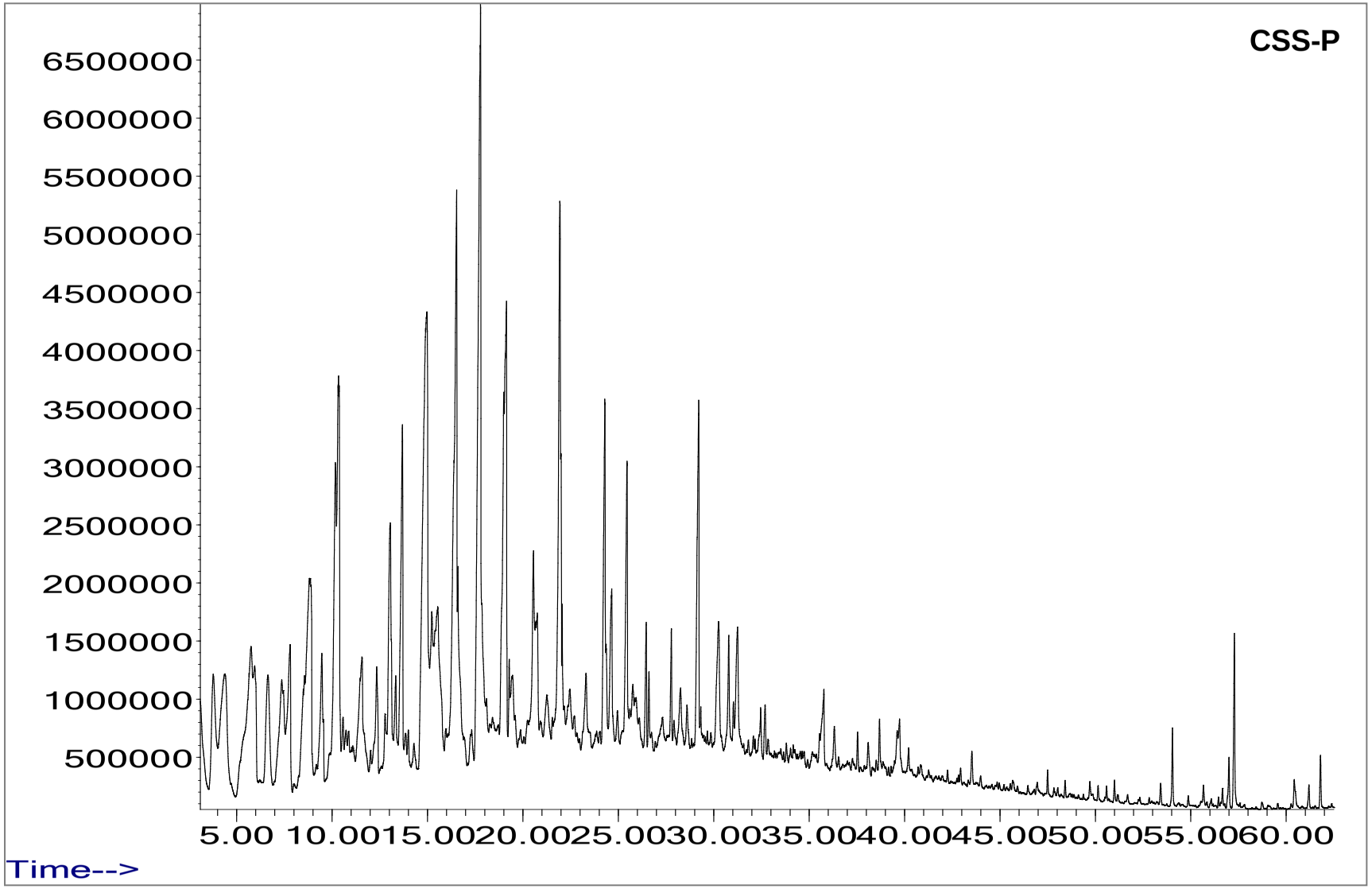
CSS-P
6500000
6000000
5500000
5000000
4500000
4000000
3500000
3000000
2500000
2000000
1500000
1000000
500000
5.00 10.00 15.00 20.00 25.00 30.00 35.00 40.00 45.00 50.00 55.00 60.00
Time-->

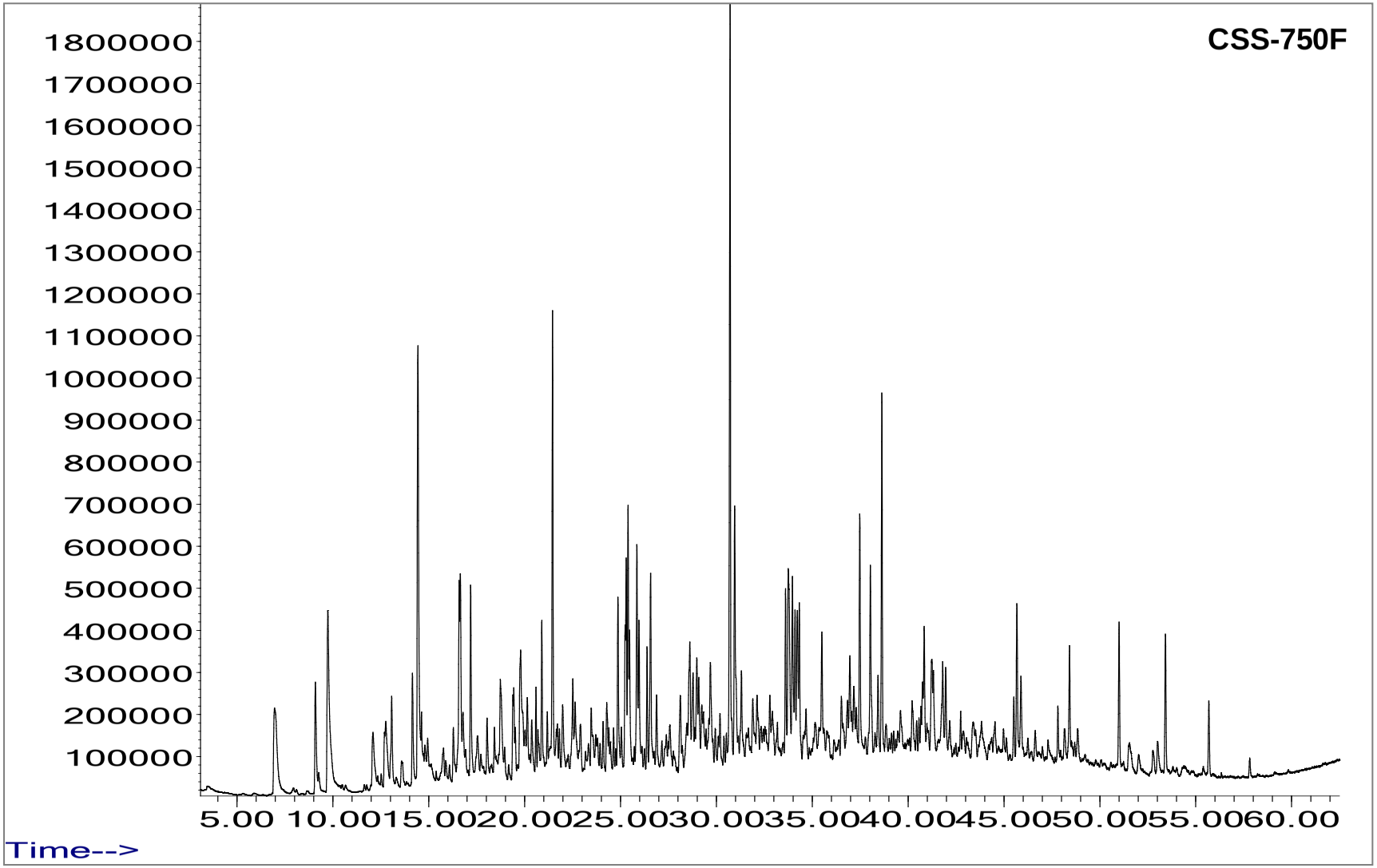
CSS-750F
1800000
1700000
1600000
1500000
1400000
1300000
1200000
1100000
1000000
900000
800000
700000
600000
500000
400000
300000
200000
100000
5.00 10.0015.0020.0025.0030.0035.0040.0045.0050.0055.0060.00
Time-->

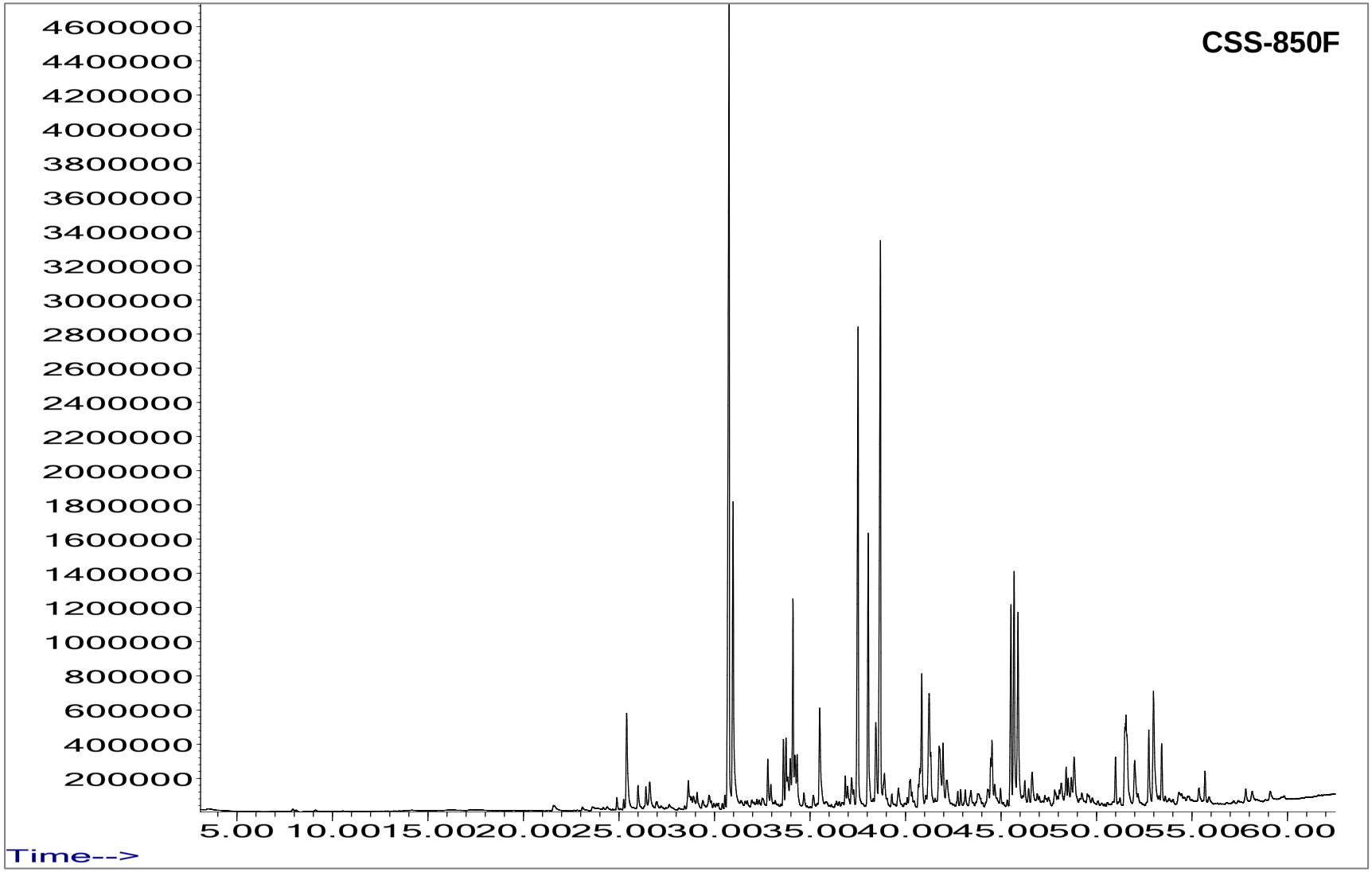
CSS-850F
4600000
4400000
4200000
4000000
3800000
3600000
3400000
3200000
3000000
2800000
2600000
2400000
2200000
2000000
1800000
1600000
1400000
1200000
1000000
800000
600000
400000
200000
5.00 10.0015.0020.0025.0030.0035.0040.0045.0050.0055.0060.00
Time-->

APPENDIX C: SEM-EDX.COMPLEMENTARY INFORMATION.

Cortaderia selloana raw materials morphology and bio-chars obtained by different pyrolysis processes. Attached graphs show the spectrum detected by the EDX of the energy released in the form of X-rays from the K orbital as well as the element type to which this energy corresponds. Tables show the percentage by weight (W%) and the atomic percentage (At%) of different chemical elements.

A) CSS

B) CSL

C) CSS-750F

D) CSS-850F

E) CSL-850F

F) CSS-P

A)

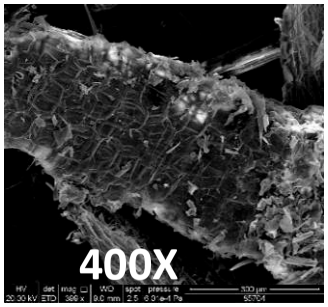

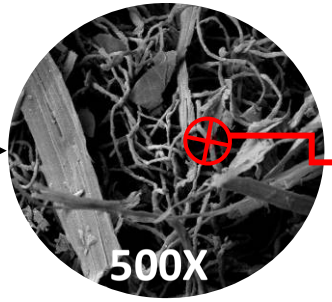

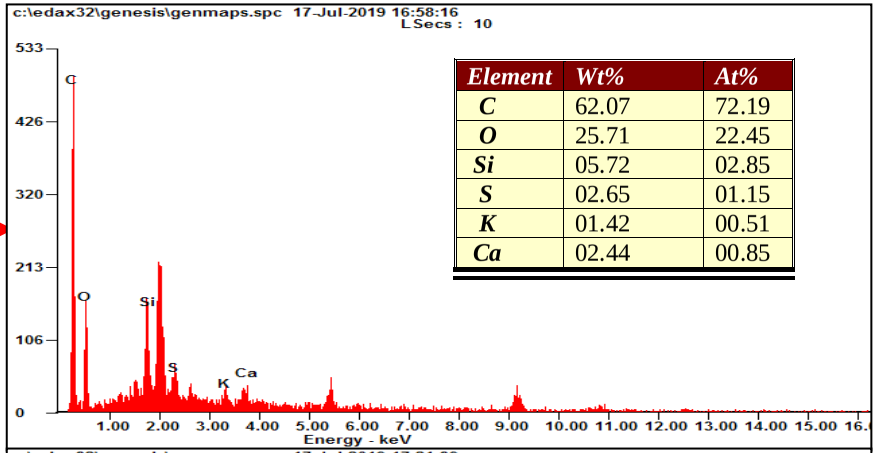

Element	Wt%	At%
C	62.07	72.19
O	25.71	22.45
Si	05.72	02.85
S	02.65	01.15
K	01.42	00.51
Ca	02.44	00.85

B)

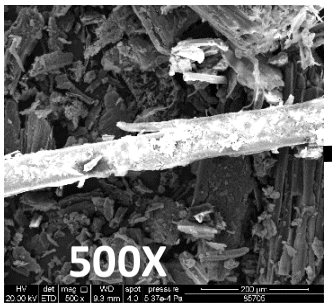

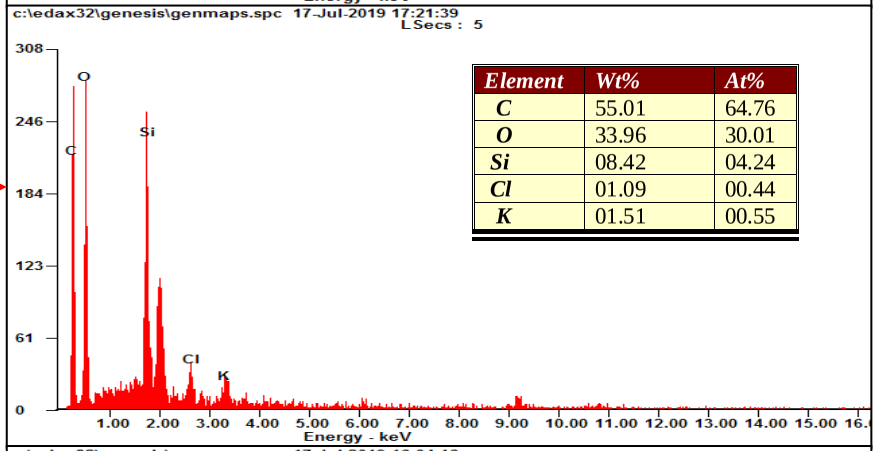

Element	Wt%	At%
C	55.01	64.76
O	33.96	30.01
Si	08.42	04.24
Cl	01.09	00.44
K	01.51	00.55

C)

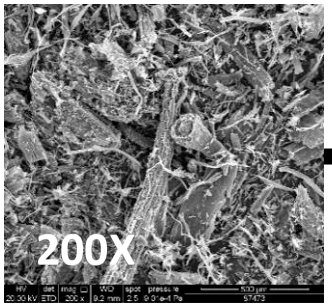

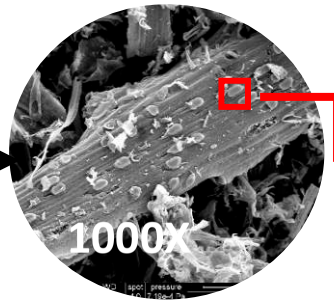

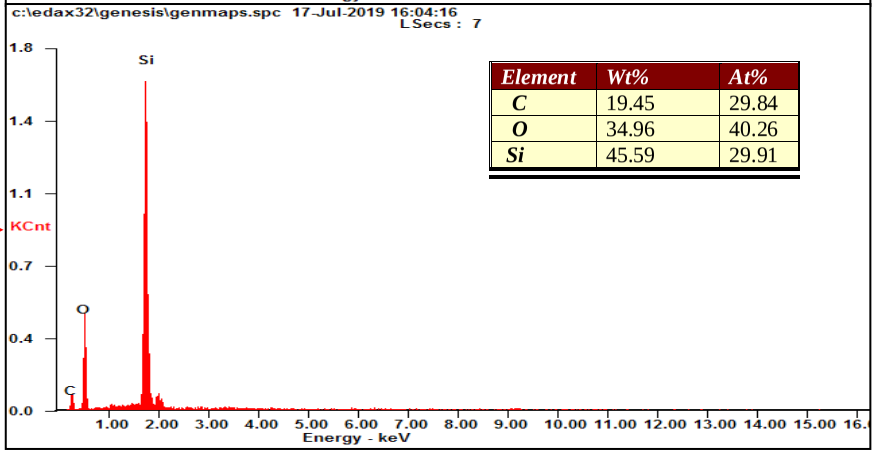

Element	Wt%	At%
C	19.45	29.84
O	34.96	40.26
Si	45.59	29.91

D)

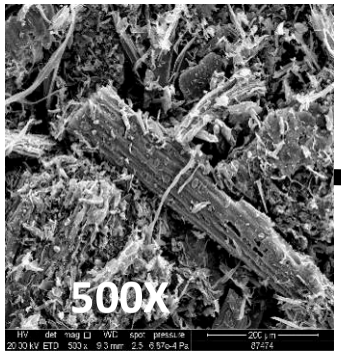

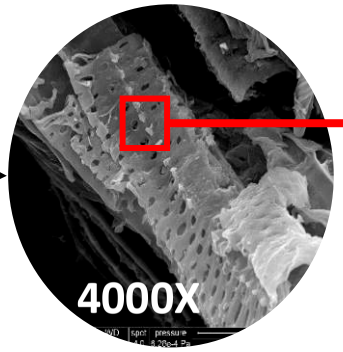

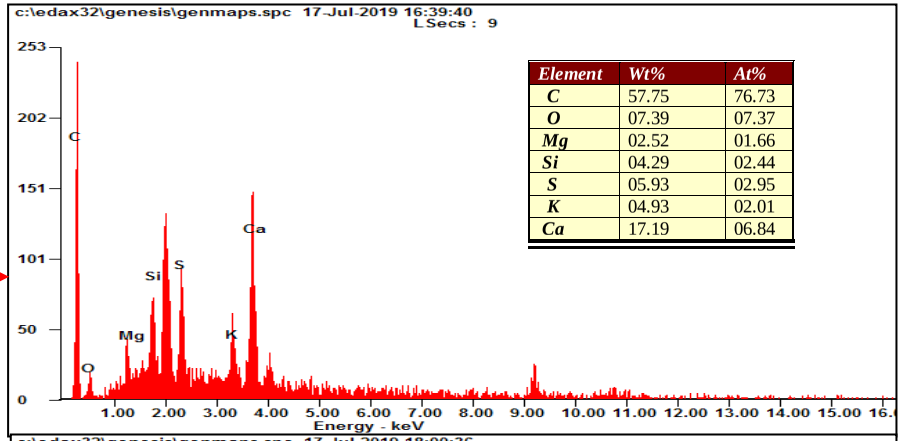

Element	Wt%	At%
C	57.75	76.73
O	07.39	07.37
Mg	02.52	01.66
Si	04.29	02.44
S	05.93	02.95
K	04.93	02.01
Ca	17.19	06.84

E)

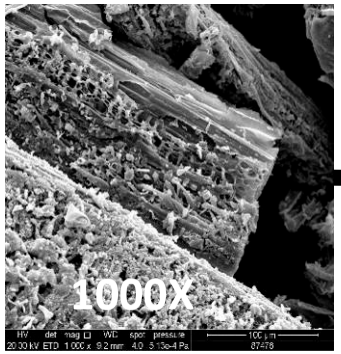

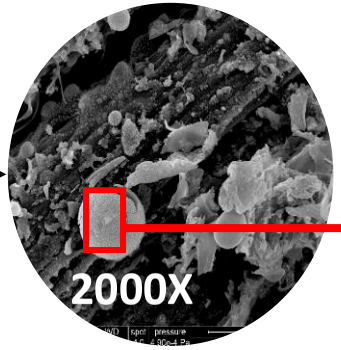

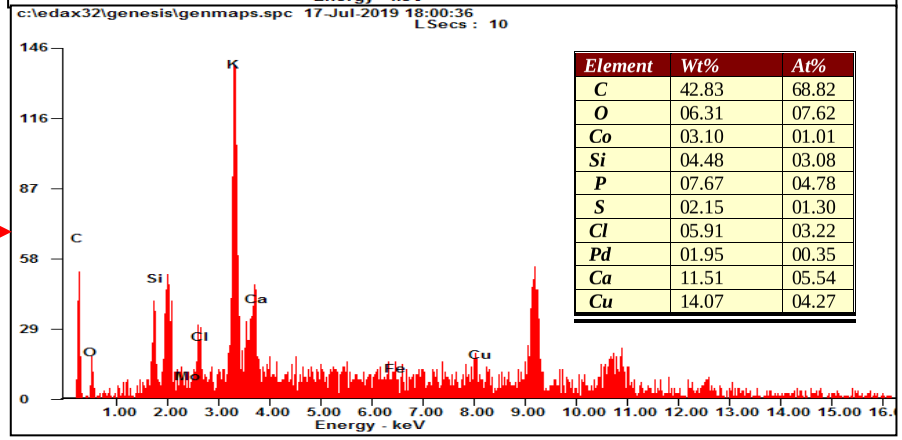

Element	Wt%	At%
C	42.83	68.82
O	06.31	07.62
Co	03.10	01.01
Si	04.48	03.08
P	07.67	04.78
S	02.15	01.30
Cl	05.91	03.22
Pd	01.95	00.35
Ca	11.51	05.54
Cu	14.07	04.27

F)

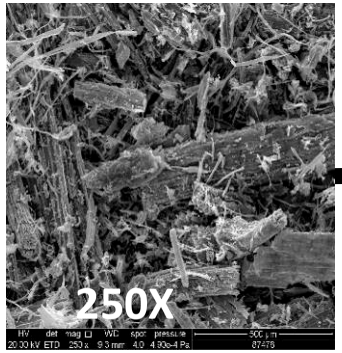

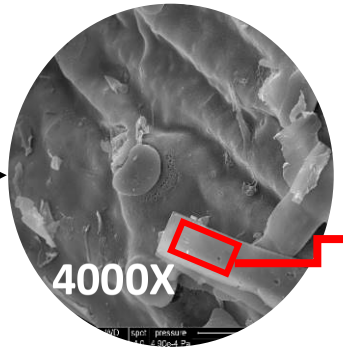

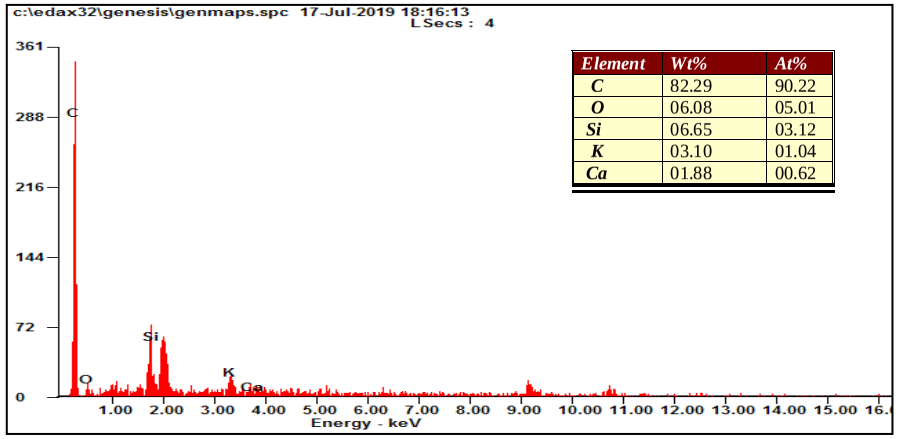

Element	Wt%	At%
C	82.29	90.22
O	06.08	05.01
Si	06.65	03.12
K	03.10	01.04
Ca	01.88	00.62